

# Newtonian gravitational constant measurement. All atomic variables become extreme when using a source mass consisting of 3 or more parts

B. Dubetsky\*  
(Dated: October 2, 2020)

Atomic interferometry methods can be used to measure the Newtonian gravitational constant. Due to symmetry factors or purposefully to improve the accuracy, the phase of an atomic interferometer can be measured at extreme values of atomic velocities and coordinates. We propose using a source mass consisting of 3 or more parts, since only in this case one can find such an arrangement of parts that all atomic variables become extreme. Nonlinear dependences of the phase on the uncertainties of atomic positions and velocities near those extreme values required us to modify the expression for the phase relative standard deviation (RSD). Moreover, taking into account nonlinear terms in the phase dependence on the atomic coordinates and velocities leads to a phase shift, which in previous experiments was also not included. A shift of 199 ppm was obtained for the experiment [1]. It reduces the value of Newtonian gravitational constant by 0.02%. In addition, it is shown that at equal sizes of the atomic cloud in the vertical and transverse directions, as well as at equal atomic vertical and transverse temperatures, systematic errors due to the finite size and temperature of the cloud disappear. The calculation also showed that when using the 13-ton source mass proposed in [2], the measurement accuracy can reach 17ppm for a source mass consisting of 4 quarters. All the consideration was carried out for the source mass consisting of a set of cylinders. An analytical expression for the gravitational field of a homogeneous cylinder is derived.

PACS numbers: 03.75.Dg; 37.25.+k; 04.80.-y

## I. INTRODUCTION

Since its birth about 40 years ago [3], the field of atom interferometry has matured significantly. The current state and prospects in this area are presented, for example, in the reviews [4] and the proposals [5–10].

Among other applications, atom interferometers (AIs) [3] are now used to measure Newtonian gravity constant  $G$  [1, 11, 12]. Searches for new schemes and options promise to increase the accuracy of these measurements. Previously, it was shown [13] that, in principle, the current state-of-art in atom interferometry would allow one to measure  $G$  with an accuracy of 200ppb. In Ref. [13] it was assumed that AIs with the best parameters achieved so far in various experiments [14–17] are used. But even for those parameter values that are currently reached in the Ref. [1, 11, 12] one can improve the accuracy of the  $G$ -measurement if it selects the appropriate positions for launching atomic clouds and the proper parameters of the sources of the gravitational field. According to [2], the main goal here is to reduce the sensitivity of the AI phase to the initial atomic coordinates. Even more important [13, 18] is the sensitivity to the launching atomic velocities.

The following procedure was used [1, 11, 13, 18]. The source mass consists of two halves, which are placed in two different configurations C and F shown in Fig 1.

We assume the notation "C and F," which was previously used in article [1]. The atomic gradiometer [19] measures the phase difference of two atomic interferom-

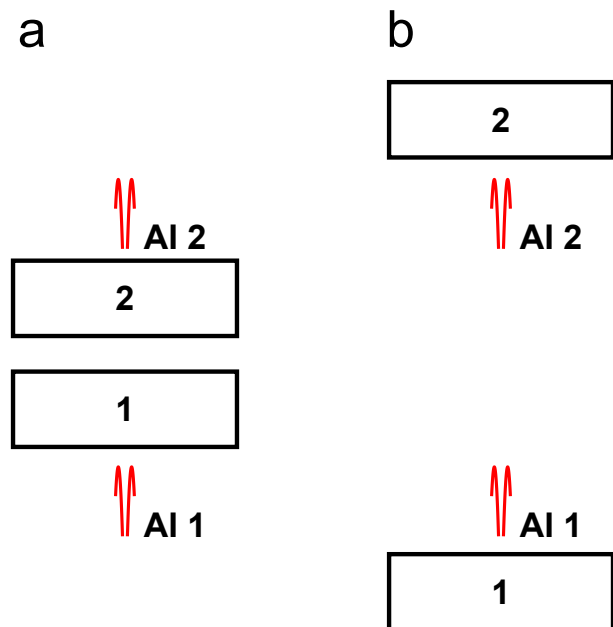


FIG. 1: Scheme of the  $G$ -measurement. The atomic gradiometer consists of two AIs. The phase difference of the AIs is measured in the presence of the gravitational field of the source mass consisting of two halves 1 and 2. Measurements are made for two configurations of the source mass "C" and "F". (a) In the C-configuration, both halves of the source mass are located between atomic clouds. (b) In the F-configuration, on the contrary, the atomic clouds are located between the halves of the source mass. Trajectories of atoms are shown in red.

\*Electronic address: bdubetsky@gmail.com

eters (AIs) 1 and 2

$$\Delta\phi^{(C,F)} = \phi^{(C,F)}(z_1, v_{z_1}) - \phi^{(C,F)}(z_2, v_{z_2}), \quad (1)$$

where  $\phi^{(C,F)}(z_j, v_j)$  is the phase of AI  $j$ , in which the atoms are launched vertically from point  $\mathbf{x}_j = (0, 0, z_j)$  at velocity  $\mathbf{v}_j = (0, 0, v_{z_j})$ . Phase difference (eq. 1) consists of two parts, the one that is induced by the gravitational field of the Earth and inertial terms and the other that is associated with the gravitational field of the source mass. One expects [1, 11, 12] that the phase double difference (PDD)

$$\Delta^{(2)}\phi = \Delta\phi^{(C)} - \Delta\phi^{(F)} \quad (2)$$

will depend only on the AI phase  $\phi_s^{(C,F)}(z_j, v_j)$  produced only by the field of source mass, and therefore can be used to measure the Newtonian gravitational constant  $G$ . Despite the fact that the gravitational field of the Earth does not affect the PDD, the gradient of this field affects [1, 11] on the accuracy of the PDD measurement. In the article [1], to reduce this influence, the mutual position of the source mass and atomic clouds are selected so that at the point of apogee of the atomic trajectories gradients of the Earth's field and the field of the source mass cancel each other. Below in Sec. III we will see that this technique only partially reduces the influence of the gravitational field of the Earth on the accuracy of the  $G$  measurement.

A different approach was used in [11]. In the  $C$ -configuration, when all the components of the source mass were located between AIs 1 and 2, for a given launching velocity

$$v_{z_1} = v_{z_2} = v, \quad (3)$$

varying the position of the atomic cloud 1, one found the point of the local maximum of the phase  $\phi^{(C)}(z_1, v)$ . Similarly, the cloud of the second interferometer was located at the point of the local minimum of the phase  $\phi^{(C)}(z_2, v)$ . In the  $F$ -configuration, one varied the positions of the source mass halves,  $h_1$  and  $h_2$ , in order to achieve a situation, when points  $(z_1, v)$  and  $(z_2, v)$  become respectively the minimum and maximum of the phase  $\phi^{(F)}(z, v)$ . After this procedure, the points  $z_1$  and  $z_2$  become extreme in both the  $C$ - and  $F$ -configurations, and therefore they are extreme for the PDD (eq. 2). The disadvantage of this approach is that the atomic velocities  $v_{z_1}$  and  $v_{z_2}$  were not varied and no extreme values were found for them.

To overcome this difficulty, we propose to divide the source mass into a larger number of parts, the position of each of which can vary independently. In the  $C$ -configuration, when all the parts are put together, under a sufficiently strong gravitational field, one can still find the points of local maximum and minimum  $(z_1, v_{z_1})$  and  $(z_2, v_{z_2})$  and place atomic clouds in those points. Our goal is that in the  $F$ -configuration the same points still

remain extreme, i.e. they satisfy a system of 4 equations

$$\partial_{z_j}\phi^{(F)}(z_j, v_{z_j}) = \partial_{v_{z_j}}\phi^{(F)}(z_j, v_{z_j}) = 0, \quad (4)$$

where  $j = 1$  or  $2$ . Although the points are given, the phase  $\phi^{(F)}(z, v)$  is a function of the coordinates of the source mass parts, such as their location along the vertical axis,  $h_1, \dots, h_n$ , where  $n$  is the number of parts. Then (eq. 4) should be considered as a system of equations for  $(h_1, \dots, h_n)$ . Since the number of equations and the number of variables must coincide, we conclude that the source mass must consist of 4 parts. However, calculations have shown that the extreme values of the velocities of both atomic clouds in the  $C$ -configuration coincide. Therefore, it is sufficient to divide the source mass into 3 parts to make extreme all atomic variables in the both configuration.

To test the feasibility of our proposals, we compared the error budgets in our case and in article [1]. In precision gravity experiments, one calculates or measures the standard deviation (SD)  $\sigma$  of the response  $f$  (such as the AI phase or phase difference) using the expression

$$\sigma(f) = \left( \sum_{m=1}^n \sigma_m^2 \right)^{1/2}, \quad (5)$$

where  $n$  is the number of variables  $\{q_1, \dots, q_n\}$ , included in the error budget,  $\sigma_m = |\partial f / \partial q_m| \sigma(q_m)$ , and  $\sigma(q_m)$  is a SD of small uncertainty in the variable  $q_m$ . We assume that variables  $\{q_1, \dots, q_n\}$  are statistically independent. See examples of such budgets in [1, 2, 11, 12, 20]. The situation changes when one considers uncertainties near the extreme points  $\{\mathbf{x}_m, \mathbf{v}_m\}$  and the signal's uncertainty becomes a quadratic function of the uncertainties of the atomic position and velocity  $\{\delta\mathbf{x}_m, \delta\mathbf{v}_m\}$ . There are several examples in which measurements were carried out (or proposed to be carried out) near extreme points. Extreme atomic coordinates were selected in the experiments [11]. Extreme atomic coordinates and velocities were found in the articles [13, 18]. The difficulties of using extreme points are noted in the article [2], where an alternative approach was proposed, based on the elimination of the dependence of the AI phase on the atomic position and velocity proposed in [21]. However, even in this case, one eliminates only the dependence on the vertical coordinates and velocities, while the transverse coordinates  $\{x_m, y_m\} = \{0, 0\}$  and velocities  $\{v_{x_m}, v_{y_m}\} = \{0, 0\}$  remain extreme. This is because the vertical component of the gravitational field of the hollow cylinder  $\delta g_3(\mathbf{x})$  is axially symmetric, and the expansion of both the field and the field gradient in transverse coordinates begins with quadratic terms. Transverse velocities and coordinates were also extreme in experiment [1]. Since for extreme variables  $\partial f / \partial q_m = 0$ , one sees that in all the cases listed above [1, 2, 11, 13, 18], the use of the expression (eq. 5) is unjustified. Revision of this expression is required. Moreover, the quadratic dependence on the uncertainties

$\{\delta\mathbf{x}_m, \delta\mathbf{v}_m\}$  leads to a shift in the signal [26]. Here, we carried out this revision and expressed both the SD and the shift of the PDD (eq. 2) in terms of the first and second derivatives of the phases  $\phi^{(C,F)}$  to find contributions to an error budget from both extreme and non-extreme variables.

Recently, we performed [13, 18] calculations, determined the optimal geometry of the gravitational field, positions and velocities of atomic clouds for the source mass of a cuboid shape. The choice of this shape is convenient for calculations since one has an analytical expression for the potential of the cuboid [22]. Despite this, it is preferable to use the source mass in a cylindrical shape to perform high-precision measurements of  $G$  [23]. Cylindrical source masses were used to measure  $G$  in [1, 11]. The hollow cylinder source mass has been proposed to achieve an accuracy of 10ppm [2]. The analytical expression for the gravitational field along the  $z$ -axis of the hollow cylinder was explored [2], but outside this axis, the potential expansion into spherical harmonics was used [1, 11]. Fast converging power series for the potential and axial component of the cylinder's gravitational field were obtained in Ref. [27]. Analytical expressions for the field of the cylinders have been derived in the articles [24, 25]. Alternatively, the technique for calculating the gravitational field without calculating the gravitational potential was proposed in the book [23], but the final expression for the cylinder field is given in [23] without derivation. Following technique [23], we calculated the field and arrived at expressions (eqs E27, E32). Our expressions do not coincide with those given in [23–25]. Both the derivations and final results are presented in this article. Following the derivations in the articles [24, 25], we are going to find out analytically the reason of the discrepancies between different expressions and publish it elsewhere.

The article is arranged as follows. Standard deviation and shift are obtained in the next section, where terms nonlinear in the atomic variables variations have been included in Sec. II A. Section II B is devoted to the AI phase and phase derivatives calculations. PDD and error budget for the scheme chosen in the article [1] are considered in the Sec. III. The 3-part source mass is considered in the Sec. IV. In the Sec. IV A, it is shown that for the same total weight of the source mass, dividing it into 3 equal parts allows one to find a scheme in which all atomic variables become extreme, and the calculation of the PDD and error budget for this scheme are carried out. In the Sec. IV B, a calculation was made for parameters suggested by G. Rossi [2]. The conclusions are given in Sec. V. Details of the numerical calculations and a derivation of the formula for the gravitational field of the cylinder are presented in the Appendixes.

## II. ERROR BUDGET NEAR EXTREME ATOMIC VARIABLES

### A. SD and shift.

Let us consider the variation of the double difference (2)

$$\begin{aligned} \delta\Delta^{(2)}\phi & [\delta\mathbf{x}_{1C}, \delta\mathbf{v}_{1C}, \delta\mathbf{x}_{2C}, \delta\mathbf{v}_{2C}; \delta\mathbf{x}_{1F}, \delta\mathbf{v}_{1F}; \delta\mathbf{x}_{2F}, \delta\mathbf{v}_{2F}] \\ & = \delta\phi^{(C)} [\delta\mathbf{x}_{1C}, \delta\mathbf{v}_{1C}] - \delta\phi^{(C)} [\delta\mathbf{x}_{2C}, \delta\mathbf{v}_{2C}] \\ & - \left[ \delta\phi^{(F)} (\delta\mathbf{x}_{1F}, \delta\mathbf{v}_{1F}) - \delta\phi^{(F)} (\delta\mathbf{x}_{2F}, \delta\mathbf{v}_{2F}) \right], \end{aligned} \quad (6)$$

where  $\{\delta\mathbf{x}_{jI}, \delta\mathbf{v}_{jI}\}$  is the uncertainty of the launching position and velocity of the cloud  $j$  ( $j = 1$  or  $2$ ) for the source mass configuration  $I$  ( $I = C$  or  $F$ ),  $\delta\phi^{(I)} (\delta\mathbf{x}_{jI}, \delta\mathbf{v}_{jI})$  is the variation of the AI  $j$  phase, produced when the source mass gravity field is in the  $I$ -configuration. For the shift  $s$  and standard deviation  $\sigma$  defined as

$$s \left( \Delta^{(2)}\phi \right) = \left\langle \delta\Delta^{(2)}\phi [\delta\mathbf{x}_{1C}, \delta\mathbf{v}_{1C}, \delta\mathbf{x}_{2C}, \delta\mathbf{v}_{2C}; \delta\mathbf{x}_{1F}, \delta\mathbf{v}_{1F}; \delta\mathbf{x}_{2F}, \delta\mathbf{v}_{2F}] \right\rangle, \quad (7a)$$

$$\begin{aligned} \sigma \left( \Delta_s^{(2)}\phi \right) & = \left\{ \left\langle \left[ \delta\Delta^{(2)}\phi (\delta\mathbf{x}_{1C}, \delta\mathbf{v}_{1C}, \delta\mathbf{x}_{2C}, \delta\mathbf{v}_{2C}; \right. \right. \right. \\ & \left. \left. \left. \delta\mathbf{x}_{1F}, \delta\mathbf{v}_{1F}; \delta\mathbf{x}_{2F}, \delta\mathbf{v}_{2F}) \right]^2 \right\rangle - s^2 \left( \Delta^{(2)}\phi \right) \right\}^{1/2} \end{aligned} \quad (7b)$$

one finds

$$\begin{aligned} s \left( \Delta^{(2)}\phi \right) & = s \left[ \phi^{(C)} (\delta\mathbf{x}_{1C}, \delta\mathbf{v}_{1C}) \right] - s \left[ \phi^{(C)} (\delta\mathbf{x}_{2C}, \delta\mathbf{v}_{2C}) \right] \\ & - s \left[ \phi^{(F)} (\delta\mathbf{x}_{1F}, \delta\mathbf{v}_{1F}) \right] + s \left[ \phi^{(F)} (\delta\mathbf{x}_{2F}, \delta\mathbf{v}_{2F}) \right], \end{aligned} \quad (8a)$$

$$\sigma \left( \Delta^{(2)}\phi \right) = \left\{ \sum_{I=C,F} \sum_{j=1,2} \sigma^2 \left[ \phi^{(I)} (\delta\mathbf{x}_{jI}, \delta\mathbf{v}_{jI}) \right] \right\}^{1/2}, \quad (8b)$$

$$s \left[ \phi^{(I)} (\delta\mathbf{x}_{jI}, \delta\mathbf{v}_{jI}) \right] = \left\langle \delta\phi^{(I)} (\delta\mathbf{x}_{jI}, \delta\mathbf{v}_{jI}) \right\rangle, \quad (8c)$$

$$\begin{aligned} \sigma \left[ \phi^{(I)} (\delta\mathbf{x}_{jI}, \delta\mathbf{v}_{jI}) \right] & = \left\{ \left\langle \left[ \delta\phi^{(I)} (\delta\mathbf{x}_{jI}, \delta\mathbf{v}_{jI}) \right]^2 \right\rangle \right. \\ & \left. - \left\langle \delta\phi^{(I)} (\delta\mathbf{x}_{jI}, \delta\mathbf{v}_{jI}) \right\rangle^2 \right\}^{1/2} \end{aligned} \quad (8d)$$

One sees that the problem is reduced to the calculation of the shift  $s$  and SD  $\sigma$  of a variation  $\delta\phi [\delta\mathbf{x}, \delta\mathbf{v}]$ . The phase of the given AI at the given configuration of the source mass comprises two parts

$$\phi (\mathbf{x}, \mathbf{v}) = \phi_E (\mathbf{x}, \mathbf{v}) + \phi_s (\mathbf{x}, \mathbf{v}), \quad (9)$$

where for the phase induced by the Earth's field, under some simplifying assumptions (see, for example, [28]),

one gets

$$\begin{aligned} \phi_E^{(I)}(\mathbf{x}, \mathbf{v}) = & \mathbf{k} \cdot \mathbf{g} T^2 + \mathbf{k} \cdot \Gamma_E T^2 [\mathbf{x} + \mathbf{v} (T + T_1)] \\ & + \mathbf{k} \cdot \Gamma_E \mathbf{g} T^2 \left( \frac{7}{12} T^2 + T T_1 + \frac{1}{2} T_1^2 \right) \end{aligned} \quad (10)$$

where  $T_1$  is the time delay between the moment the atoms are launched and the 1st Raman pulse. For the vertical wave vector  $\mathbf{k} = (0, 0, k)$ , expanding (eq. 9) to the second order terms one gets

$$\begin{aligned} \delta\phi(\delta\mathbf{x}, \delta\mathbf{v}) = & \left( \tilde{\gamma}_{xm} + \frac{\partial\phi_s}{\partial x_m} \right) \delta x_m + \left( \tilde{\gamma}_{vm} + \frac{\partial\phi_s}{\partial v_m} \right) \delta v_m \\ & + \frac{1}{2} \frac{\partial^2\phi_s}{\partial x_m \partial x_n} \delta x_m \delta x_n + \frac{1}{2} \frac{\partial^2\phi_s}{\partial v_m \partial v_n} \delta v_m \delta v_n \\ & + \frac{\partial^2\phi_s}{\partial x_m \partial v_n} \delta x_m \delta v_n, \end{aligned} \quad (11)$$

where

$$\tilde{\gamma}_{xm} = k \Gamma_{E3m} T^2; \quad (12a)$$

$$\tilde{\gamma}_{vm} = (T + T_1) \tilde{\gamma}_{xm}, \quad (12b)$$

where  $\Gamma_{E3m}$  is the  $3m$ -component of the Earth's field gravity-gradient tensor. A summation convention implicit in (eq. 11) will be used in all subsequent equations. Repeated indices and symbols appearing on the right-hand-side (rhs) of an equation are to be summed over, unless they also appear on the left-hand-side (lhs) of that equation. Let assume that the distribution functions of the uncertainties are sufficiently symmetric, and all odd moments are equal 0. The moments of the second and fourth orders are given by

$$\langle \delta q_m \delta q_n \rangle = \delta_{mn} \sigma^2(q_m), \quad (13a)$$

$$\begin{aligned} \langle \delta q_m \delta q_n \delta q_{m'} \delta q_{n'} \rangle = & \delta_{mn} \delta_{m'n'} \sigma^2(q_m) \sigma^2(q_{m'}) \\ & + (\delta_{mm'} \delta_{nn'} + \delta_{mn'} \delta_{nm'}) \sigma^2(q_m) \sigma^2(q_n) \\ & + \delta_{mn} \delta_{mm'} \delta_{mn'} \kappa(q_m) \sigma^4(q_m), \end{aligned} \quad (13b)$$

where  $q_i$  is either a position  $x_i$  or a velocity  $v_i$ ,  $\sigma(q_i)$  is SD of the uncertainty  $\delta q_i$ ,  $\delta_{mn}$  is Kronecker symbol,  $\kappa(q_m)$  is a cumulant of the given uncertainty  $\delta q_m$ , defined as

$$\kappa(q_m) = \frac{\langle \delta q_m^4 \rangle}{\sigma^4(q_m)} - 3. \quad (14)$$

Let assume also that uncertainties of the launching velocities and positions are statistically independent,

$$\langle \delta x_m \delta v_n \rangle = 0. \quad (15)$$

Using the moments (eqs. 13, 15) one arrives at the following expressions for the SD and shift

$$\begin{aligned} \sigma[\phi(\delta\mathbf{x}, \delta\mathbf{v})] = & \left\{ \left( \tilde{\gamma}_{xm} + \frac{\partial\phi_s}{\partial x_m} \right)^2 \sigma^2(x_m) \right. \\ & + \left( \tilde{\gamma}_{vm} + \frac{\partial\phi_s}{\partial v_m} \right)^2 \sigma^2(v_m) \\ & + \frac{1}{2} \left[ \left( \frac{\partial^2\phi}{\partial x_m \partial x_n} \right)^2 \sigma^2(x_m) \sigma^2(x_n) \right. \\ & \left. \left. + \left( \frac{\partial^2\phi}{\partial v_m \partial v_n} \right)^2 \sigma^2(v_m) \sigma^2(v_n) \right] \right. \\ & + \left( \frac{\partial^2\phi}{\partial x_m \partial v_n} \right)^2 \sigma^2(x_m) \sigma^2(v_n) \\ & + \frac{1}{4} \left[ \left( \frac{\partial^2\phi}{\partial x_m^2} \right)^2 \kappa(x_m) \sigma^4(x_m) \right. \\ & \left. \left. + \left( \frac{\partial^2\phi}{\partial v_m^2} \right)^2 \kappa(v_m) \sigma^4(v_m) \right] \right\}^{1/2}, \quad (16a) \\ s[\phi(\delta\mathbf{x}, \delta\mathbf{v})] = & \frac{1}{2} \left( \frac{\partial^2\phi}{\partial x_m^2} \sigma^2(x_m) + \frac{\partial^2\phi}{\partial v_m^2} \sigma^2(v_m) \right), \quad (16b) \end{aligned}$$

One sees that, even for the symmetric uncertainties distribution, the knowledge of the uncertainties' SDs is not sufficient. One has to know also uncertainties' cumulants (eq. 14). The exclusion here is Gaussian distributions, for which the cumulants

$$\kappa(x_m) = \kappa(v_m) = 0. \quad (17)$$

Further calculations will be performed only for these distributions.

For the each case considered below we are going to calculate the double difference (eq. 2) and relative contributions to the SD (eq. 16a) and shift (eq. 16b) from the each of two atom clouds at the each of two source mass configurations.

## B. The phase and phase derivatives of the atom interferometer

To calculate the phase  $\phi_s^{(I)}$  produced by the gravitational field of the source mass, we use the results obtained in the article [29]. It is necessary to distinguish three contributions to the phase, classical, quantum, and Q-term (see Eqs. (62c, 64, 60c), (62d, 71, 60c), (89) in [29] for these three terms). The quantum term arises from the quantum kicks  $\pm \hbar \mathbf{k}$  of the atomic momentum when interacting with the Raman pulse, while the Q-term is due to quantum corrections to the free evolution of the density matrix in the Wigner representation in the space between Raman pulses.

For Q-term an estimate was obtained

$$\frac{\phi_Q}{\phi_s^{(I)}} \sim \frac{1}{24} \left( \frac{\hbar k T}{L M_a} \right)^2, \quad (18)$$

where  $M_a$  is the atom mass,  $L$  is the characteristic distance over which the gravitational potential of the test mass changes. For  $^{87}\text{Rb}$ , at  $L > 0.3\text{m}$ , the relative weight of the Q-term does not exceed 2ppb, and we neglect it. For the remaining terms and the vertical effective wave vector,  $\mathbf{k} = \{0, 0, k\}$ , one gets

$$\phi_s^{(I)}(\mathbf{x}, \mathbf{v}) = k \int_0^T dt [(T-t) \delta g_3(\mathbf{a}(T+t)) + t \delta g_3(\mathbf{a}(t))], \quad (19)$$

where

$$\mathbf{a}(t) = \mathbf{x} + \mathbf{v}(T_1 + t) + \frac{1}{2} \mathbf{g}(T_1 + t)^2 + \mathbf{v}_r t, \quad (20)$$

the recoil velocity is given by

$$\mathbf{v}_r = \hbar \mathbf{k} / 2M_a, \quad (21)$$

$\delta g_3(\mathbf{x})$  is the vertical component of the gravitational field of the source mass. The derivatives of this phase of the first and second order are given by

$$\frac{\partial \phi_s^{(I)}(\mathbf{x}, \mathbf{v})}{\partial x_m} = k \int_0^T dt [(T-t) \Gamma_{s3m}(\mathbf{a}(T+t)) + t \Gamma_{s3m}(\mathbf{a}(t))], \quad (22a)$$

$$\frac{\partial \phi_s^{(I)}(\mathbf{x}, \mathbf{v})}{\partial v_m} = k \int_0^T dt [(T-t)(T_1 + T + t) \times \Gamma_{s3m}(\mathbf{a}(T+t)) + t(T_1 + t) \Gamma_{s3m}(\mathbf{a}(t))], \quad (22b)$$

$$\frac{\partial^2 \phi_s^{(I)}(\mathbf{x}, \mathbf{v})}{\partial x_m \partial x_n} = k \int_0^T dt [(T-t) \chi_{s3mn}(\mathbf{a}(T+t)) + t \chi_{s3mn}(\mathbf{a}(t))], \quad (22c)$$

$$\frac{\partial^2 \phi_s^{(I)}(\mathbf{x}, \mathbf{v})}{\partial x_m \partial v_n} = k \int_0^T dt [(T-t)(T_1 + T + t) \times \chi_{s3mn}(\mathbf{a}(T+t)) + t(T_1 + t) \chi_{s3mn}(\mathbf{a}(t))], \quad (22d)$$

$$\frac{\partial^2 \phi_s^{(I)}(\mathbf{x}, \mathbf{v})}{\partial v_m \partial v_n} = k \int_0^T dt [(T-t)(T_1 + T + t)^2 \times \chi_{s3mn}(\mathbf{a}(T+t)) + t(T_1 + t)^2 \chi_{s3mn}(\mathbf{a}(t))], \quad (22e)$$

where  $\Gamma_{s3m}(\mathbf{x}) = \frac{\partial \delta g_3(\mathbf{x})}{\partial x_m}$  is the  $3m$ -component of the gravity-gradient tensor of the source mass field, and

$$\chi_{s3mn}(\mathbf{x}) = \frac{\partial^2 \delta g_3(\mathbf{x})}{\partial x_m \partial x_n} \quad (23)$$

is the  $3mn$ -component of the curvature tensor of this field.

In these expressions, any points on the atomic trajectory can be chosen as atomic variables, i.e. the (eqs. 10,

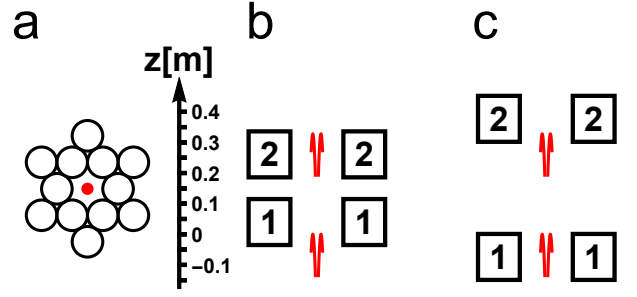


FIG. 2: The mutual positioning of the source mass halves 1 and 2, and atomic clouds. Top view (a), cross-sections  $x = 0$  for  $C$ -configuration (b) and  $F$ -configuration (c).

19, 22) are invariant under replacement

$$\{\vec{x}, \vec{v}\} \rightarrow \{\vec{x}', \vec{v}'\} = \left\{ \vec{x} + \vec{v}T' + \frac{1}{2} \vec{g}T'^2, \vec{v} + \vec{g}T' \right\} \quad (24a)$$

$$T_1 \rightarrow T_1 - T'. \quad (24b)$$

This freedom of choice allowed in Ref. [1] the apogee of the atomic trajectory in the lower interferometer to be used as a reference point. However, the situation changes when one builds an error budget. If the atomic coordinates and velocities are statistically independent at the launch point, then this independence is violated at all other points, since at them  $\delta \vec{x}' = \delta \vec{x} + T' \delta \vec{v}$ , and, consequently, instead of (eq. 15) one gets

$$\langle \delta x'_m \delta v'_n \rangle = \delta_{mn} \sigma^2(v_m) T' \neq 0. \quad (25)$$

Since statistical independence is necessary for calculating the error budget using both the generally accepted (eq. 5) and (eq. 16a), the launch point should be preferred for calculations. We did not find information about the delay time  $T_1$  between the moment of atom launch and the first Raman pulse. An example of calculating the AI phase at  $T_1 \neq 0$  can be found in the article [18]. In this article, all calculations are made under the assumption that

$$T_1 \ll T. \quad (26)$$

### III. CORRECTIONS TO THE FORMER ERROR BUDGET.

We applied the formula for the cylinder field (eq. E27) to calculate the phases produced by different sets of cylinders. In this section, we consider the field geometry chosen in the article [1], see Fig. 2.

Two halves of the source mass, each including 12 tungsten alloy cylinders, move in a vertical direction from  $C$ -configuration to  $F$ -configuration, in each of which one measures the phase difference of the first order (eq. 1), and then PDD (eq. 2). The following system parameters are important for calculation: cylinder density  $\rho = 18263 \text{kg/m}^3$ , cylinder radius and height

$R = 0.04995\text{m}$  and  $h = 0.15011\text{m}$ , Newtonian gravitational constant  $G = 6.67430 \cdot 10^{-11}\text{kg}^{-1}\text{m}^3\text{s}^{-2}$  [30], the Earth's gravitational field  $g = 9.80492\text{m/s}^2$  [31], the delay between impulses  $T = 160\text{ms}$ , the effective wave vector  $k = 1.61058 \cdot 10^7\text{m}^{-1}$ , the mass of the  $^{87}\text{Rb}$   $M_a = 86.9092\text{a.u.}$  [32], atomic velocity at the moment of the first impulse action  $v = 1.62762\text{m/s}$  [33]. With respect to the apogee of the atomic trajectory in the lower interferometer, the  $z$ -coordinates of the centers of the halves of the source mass are equal to  $0.04\text{m}$  and  $0.261\text{m}$  in the  $C$ -configuration and  $-0.074\text{m}$  and  $0.377\text{m}$  in the  $F$ -configuration,  $z$ -coordinate of the atomic trajectory apogee in the upper interferometer is equal to  $0.328\text{m}$  (see Fig. 2b,c). Using (eq. 19) we got for PDD

$$\Delta^{(2)}\phi = 0.530552\text{rad}, \quad (27)$$

which is less than the value obtained in the article [1], by 3.2%. The difference seems to be related to the fact that in our calculations, the contributions from platforms and other sources of gravity were not taken into account. Details of the calculations of the error budget one can find in Appendix A. For SDs achieved in [1]

$$\sigma(x_{jI}) = \sigma(y_{jI}) = 10^{-3}\text{m}, \quad (28a)$$

$$\sigma(z_{jI}) = 10^{-4}\text{m}, \quad (28b)$$

$$\sigma(v_{xjI}) = \sigma(v_{yjI}) = 6 \cdot 10^{-3}\text{m/s}, \quad (28c)$$

$$\sigma(v_{zjI}) = 3 \cdot 10^{-3}\text{m/s}, \quad (28d)$$

using Eqs. (eq. A2) one arrives to the RSD and the shift

$$\sigma(\delta\Delta_s^{(2)}\phi) = 275\text{ppm} [1 + 6.14 \cdot 10^{13} (\Gamma_{E31}^2 + \Gamma_{E32}^2)]^{1/2}, \quad (29a)$$

$$s(\delta\Delta_s^{(2)}\phi) = 199\text{ppm}. \quad (29b)$$

The non-diagonal matrix elements of the gradient tensor of the Earth's field consist of three contributions arising from the fact that the Geoid is not spherical, from the rotation of the Earth, and from the anomalous part of the field. The first two contributions were taken into account exactly [35], and they are 3 orders of magnitude smaller than the diagonal element  $\Gamma_{E33}$ . We failed to find any information about the anomalous part of the Earth's gravitational field. However, it is seen that the non-diagonal elements of the tensor can be neglected with an accuracy of not more than 10% if

$$\sqrt{\Gamma_{E31}^2 + \Gamma_{E32}^2} < 58.5E. \quad (30)$$

#### IV. SOURCE MASS CONSISTING OF 3 PARTS.

##### A. Using current parameters [1]

In this paper, we propose to divide the source mass not into two halves (as in the article [1]), but into 3 parts.

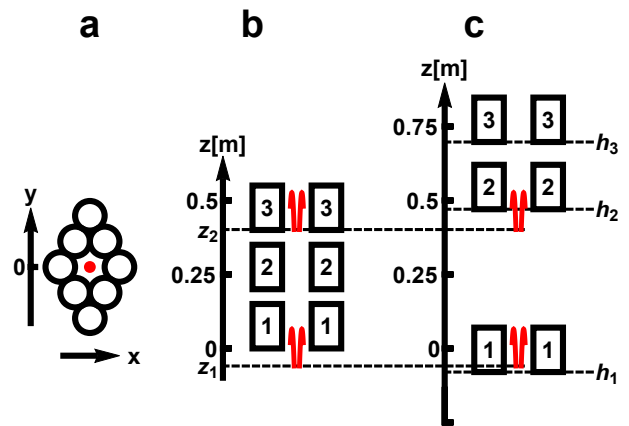


FIG. 3: The same as Fig. 2 but for the source mass consisting of 3 parts

The calculation showed that even in this case, 24 cylinders are enough for the gradient of the source mass gravitational field to compensate the gradient of the Earth's field. A symmetrical in the horizontal plane configuration of the source mass is shown in Fig. 3.

In a  $C$ -configuration, according to [11] and unlike [1] we have chosen for calculations in this section the distance between the lower and upper set of cylinders  $dh = 0.05\text{m}$ . One could use the local maximum and minimum of the phase (eq. 9) in the coordinate and velocity space

$$z_1 = -0.059\text{m}, z_2 = 0.402\text{m}, v_{z1} = v_{z2} = v = 1.563\text{m/s}, \quad (31)$$

from which atomic clouds of the 1st and 2nd AI should be launched. The phases of the interferometers (eq. 19) will be equal

$$\{\phi_s^{(C)}(z_1, v), \phi_s^{(C)}(z_2, v)\} = \{0.144901\text{rad}, -0.150482\text{rad}\}. \quad (32)$$

One should underline that the extrema (eq. 31) are different from the absolute maxima and minima of the phase  $\phi_s^{(C)}(z, v)$ , which were previously considered for the cuboid source mass in the Refs. [13, 18].

The launching velocity in (eq. 31) is close to the velocity of the atomic fountain [36]  $gT$ . differing from it only in the third digit,

$$\delta v = v - gT \approx -5.8 \cdot 10^{-3}\text{m/s}. \quad (33)$$

From (eqs. 41, D5a, D8a) one sees that deviation  $\delta v$  could only slightly depend on the interrogation time  $T$ . The difference (eq. 33), however, is sufficient to exclude the parasitic signal [37], which occurs when atoms interact with a Raman pulse having an opposite sign of the effective wave vector. Indeed, the Raman frequency detuning for the parasitic signal  $\delta = 2k\delta v \approx -2 \cdot 10^5\text{s}^{-1}$ . If the duration of the  $\pi$ -pulse  $\tau \sim 60\mu\text{s}$ , then the absolute value of the detuning  $\delta$  is an order of magnitude greater than the inverse pulse duration, and the proba-

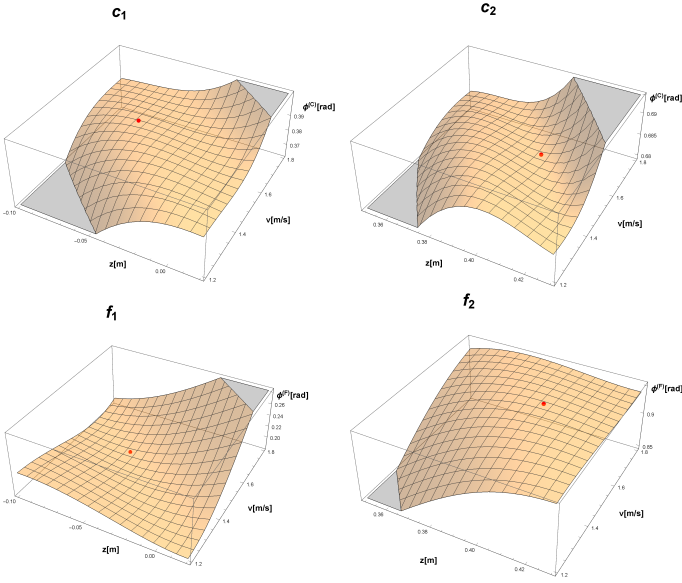


FIG. 4: Phases of AIS 1 and 2 in the vicinity of points  $\{z_1, v\}$  and  $\{z_2, v\}$ , given in (eq. 31) for  $C$ - and  $F$ -configurations of the source mass. In the expression for the phase, we kept only the terms that depend on the vertical components of the atomic coordinates and velocities, i.e., we put that  $\phi^{(C,F)}(z, v) = k\Gamma_{E33}T^2[z + v(T + T_1)] + \phi_s^{(C,F)}(z, v)$ . Extrema are shown in red. One sees that the point  $\{z_1, v\}$  is maximum in  $C$ -configuration and minimum in  $F$ -configuration and, on the contrary, the point  $\{z_2, v\}$  is the minimum in  $C$ -configuration and maximum in  $F$ -configuration.

bility of excitation of atoms by a parasitic Raman field is negligible, is estimated to be about 4%.

Let us now consider the  $F$ -configuration, see Fig. 3c. We are looking for an arrangement of parts of the source mass where the points (31) are still extremes, i.e. the coordinates of the parts of the source mass  $\{h_1, h_2, h_3\}$  are the roots of a system of 4 equations (eq. 4) with a constraint (eq. 3). There can be at least 2 such solutions. We have found and offer it for use a numerical solution

$$\{h_1, h_2, h_3\} = \{-0.080\text{m}, 0.470\text{m}, 0.697\text{m}\}, \quad (34)$$

when the point  $\{z_1, v\}$  becomes the local minimum, and the point  $\{z_2, v\}$  becomes the local maximum of the AI phase,

$$\{\phi_s^{(F)}(z_1, v), \phi_s^{(F)}(z_2, v)\} = \{-0.065580\text{rad}, 0.107651\text{rad}\} \quad (35)$$

Using (eqs. 1, 2, 32, 35) one gets for PDD

$$\Delta^{(2)}\phi = 0.468614\text{rad}. \quad (36)$$

The dependencies of the AIS phase (eq. 10) near the extremes are shown in Fig. 4.

Details of the calculations of the error budget one can find in Appendix B. For SDs (eq. 28) achieved in [1]

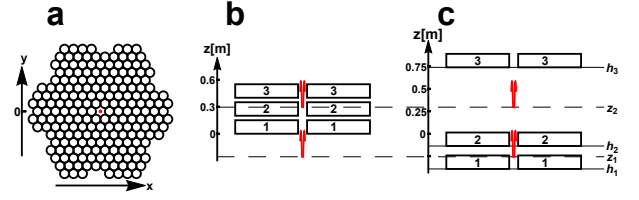


FIG. 5: The same as Fig. 3 but for the 13-ton source mass.

using (eqs.B3) one arrives to the RSD and the shift

$$\sigma(\delta\Delta^{(2)}\phi) = 75\text{ppm} [1 + 1.05 \cdot 10^{-15} (\Gamma_{E31}^2 + \Gamma_{E32}^2)]^{1/2}, \quad (37a)$$

$$s(\delta\Delta^{(2)}\phi) = 120\text{ppm}. \quad (37b)$$

The non-diagonal elements of the gravity-gradient tensor of the Earth field,  $\Gamma_{E31}$  and  $\Gamma_{E32}$ , can be neglected with an accuracy of not more than 10% if

$$\sqrt{\Gamma_{E31}^2 + \Gamma_{E32}^2} < 6.5E. \quad (38)$$

## B. Using suggested G. Rossi parameters [2]

We have already mentioned above that G. Rosi proposed and studied [2] a new approach to the measurement of  $G$  with an accuracy of 10 ppm, based on the technique of eliminating the gravity-gradient terms [21]. In addition to the new technique, estimates have been performed for the source mass weight increased to the 13 tons, time separation between Raman pulses increased to

$$T = 243\text{ms}, \quad (39)$$

and the uncertainty of the velocity of atomic clouds reduced to

$$\sigma(v_{xjI}) = \sigma(v_{yjI}) = 2\text{mm/s}, \quad (40a)$$

$$\sigma(v_{zjI}) = 0.3\text{mm/s}. \quad (40b)$$

In this section, we tested our method of dividing the source mass into 3 parts for parameters close to those proposed in [2] and for the source mass consisting of cylinders used in [1]. We chose the location of the cylinders on 3 floors shown in Fig. 5. It is easy to see that the cylinders are still positioned symmetrically in the horizontal plane, and their total weight only slightly exceeds 13 tons. This arrangement of the cylinders is a natural generalization of the geometry chosen in the [1].

In a  $C$ -configuration, one could use the local maximum and minimum of the phase (eq. 9) in the coordinate and velocity space

$$z_1 = -0.257\text{m}, z_2 = 0.296\text{m}, v_{z1} = v_{z2} = v = 2.377\text{m/s}, \quad (41)$$

from which it is necessary to launch atomic clouds of the 1st and 2nd AI. The phases of the interferometers (eq. 19) will be equal

$$\left\{ \phi_s^{(C)}(z_1, v), \phi_s^{(C)}(z_2, v) \right\} = \{1.61119\text{rad}, -1.53732\text{rad}\}. \quad (42)$$

Let us now consider the  $F$ -configuration, see Fig. 5c. We are looking for an arrangement of parts of the source mass where the points (eq. 31) are still extremes, i.e. the coordinates of the parts of the source mass  $\{h_1, h_2, h_3\}$  are the roots of a system of 4 equations (eq. 4) with a constraint (eq. 3). There can be at least 2 such solutions. We have found and offer it for use a numerical solution

$$\{h_1, h_2, h_3\} = \{-0.377\text{m}, -0.153\text{m}, 0.561\text{m}\}, \quad (43)$$

when the point  $\{z_1, v\}$  becomes the local minimum, and the point  $\{z_2, v\}$  becomes the local maximum of the AI phase,

$$\left\{ \phi_s^{(F)}(z_1, v), \phi_s^{(F)}(z_2, v) \right\} = \{-0.724326\text{rad}, -0.015028\text{rad}\}. \quad (44)$$

Using (eqs. 1, 2, 32, 35) one gets for PDD

$$\Delta^{(2)}\phi = 3.85782\text{rad}. \quad (45)$$

Details of the calculations of the error budget one can find in Appendix C. For SDs (eqs. 28a, 28b, 40) using (eqs. C4) one arrives to the RSD and the shift

$$\sigma\left(\delta\Delta^{(2)}\phi\right) = 23\text{ppm} \left[1 + 5.84 \cdot 10^{14} (\Gamma_{E31}^2 + \Gamma_{E32}^2)\right]^{1/2}, \quad (46a)$$

$$s\left(\delta\Delta^{(2)}\phi\right) = 45\text{ppm}. \quad (46b)$$

The non-diagonal elements of the gravity-gradient tensor of the Earth field,  $\Gamma_{E31}$  and  $\Gamma_{E32}$ , can be neglected with an accuracy of not more than 10% if

$$\sqrt{\Gamma_{E31}^2 + \Gamma_{E32}^2} < 19\text{E}. \quad (47)$$

## V. CONCLUSION

This article is devoted to the calculation of the error budget in the measurement of the Newtonian gravitational constant  $G$  by atomic interferometry methods. Using the technique [23], we obtained expressions for the gravitational field of the cylinder, which is used in these measurements.

Despite the compensation of the gradient of the Earth gravitational field at the points of apogees of the atomic trajectories achieved in the article [1], an absence of this compensation along the entire trajectory leads to the influence of the Earth's field on the  $G$  measurement accuracy. To overcome this influence, we propose to use source mass divided on 3 or more parts

The main attention in this article is paid to the calculation of standard deviation (SD) and the shift of the PDD due to the uncertainties of the mean values of the initial coordinates and the velocities of atomic clouds  $\{\delta\mathbf{x}, \delta\mathbf{v}\}$ . We propose to include in the error budget new terms. They are originated from the quadratic dependence of the variation of the AI phases on  $\{\delta\mathbf{x}, \delta\mathbf{v}\}$ . The shift arises only after including those terms. At the conditions realized in the article [1], calculations brings us to the shift (eq. 29b) and to the opposite relative correction  $\Delta G/G = -199\text{ppm}$ , which is larger than corrections considered in [1]. After including this correction, the value of the gravitational constant  $G$  should be shifted to

$$G = 6.67058 * 10^{-11} \text{m}^3 \text{kg}^{-1} \text{s}^{-2} \quad (48)$$

from the value  $G = 6.67191 * 10^{-11} \text{m}^3 \text{kg}^{-1} \text{s}^{-2}$  measured in [1]. Monte Carlo simulation was used in [1] to determine the constant  $G$ . In principle, if one includes in the simulation the variations in the spatial centers of atomic clouds and the centers of the atomic velocity distribution, the shift (eq. 29b) would be included in the averaging over random samples of the atomic coordinates and velocities. However, these variations, according to [1], were not included in the Monte Carlo simulation, which allows us to suggest shifting the measurement result of the constant  $G$  to the value (eq. 48).

Another discrepancy with article [1] is the measurement accuracy. According to our calculation for the atomic coordinates' and velocities' SDs (eq. 28), which were achieved in [1], the measurement accuracy of  $G$  should not be less than 275ppm, see Eq. (eq. 29a), while according to [1] the total accuracy was 148ppm.

We propose to generalize the method [11] as follows. In the  $C$ -configuration, when all the parts of the source mass are pieced together, we look for local extremes of the total phase of the atomic interferometer (eq. 9), using the (eqs. 10, 19-21). In addition to the atomic coordinates, which were varied in [11], we vary also the atomic velocities. Calculations have shown that the atomic velocities at the points of local maximum and minimum coincide. The task now is to ensure that these found points remain extreme in the  $F$ -configuration. At the same time, in order for the contribution to the PDD from the  $F$ -configuration to be positive, the former maximum point  $(z_1, v_{z_1})$  must become the minimum point, and the former minimum point  $(z_2, v_{z_2})$  must become the maximum point. The necessary condition for this is that the phase of the atomic interferometer, as a function of the positions of the source mass parts, must satisfy a system of 4 equations (eq. 4) with a restraint (eq. 3), i.e., at least, the phase must be a function of 3 parameters of the source mass. In contrast to [1, 11], we propose to divide it into 3 parts, and to choose for the parameters the 3 vertical coordinates of the source mass parts  $\{h_1, h_2, h_3\}$ .

We considered this procedure in Section IV for the same number of cylinders as in [1, 11]. **In fact, it is shown that a simple redistribution of the cylin-**

TABLE I: Error budgets summaries for different numbers of the source mass parts and different numbers of cylinders. We neglect contribution to the RSD from the non diagonal matrix elements of the Earth's field gravity-gradient tensor. Budgets in the columns 3-5,7,8 are built in this article.

Number of source mass parts	2	2	3	4	1	3	4
Source mass [kg]	516	516	516	688	13000	13022	13065
Uncertainty of the vertical position $\sigma(z_{jI})$ [m]	$10^{-4}$	$10^{-4}$	$10^{-4}$	$10^{-4}$	$10^{-4}$	$10^{-4}$	$10^{-4}$
Uncertainty of the horizontal position $\sigma(x_{jI}) = \sigma(y_{jI})$ [m]	$10^{-3}$	$10^{-3}$	$10^{-3}$	$10^{-3}$	$10^{-3}$	$10^{-3}$	$10^{-3}$
Uncertainty of the vertical velocity $\sigma(v_{zjI})$ [m/s]	$3 \cdot 10^{-3}$	$3 \cdot 10^{-3}$	$3 \cdot 10^{-3}$	$3 \cdot 10^{-3}$	$2 \cdot 10^{-3}$	$2 \cdot 10^{-3}$	$2 \cdot 10^{-3}$
Uncertainty of the horizontal velocity $\sigma(v_{xjI}) = \sigma(v_{yjI})$ [m/s]	$6 \cdot 10^{-3}$	$6 \cdot 10^{-3}$	$6 \cdot 10^{-3}$	$6 \cdot 10^{-3}$	$3 \cdot 10^{-4}$	$3 \cdot 10^{-4}$	$3 \cdot 10^{-4}$
Interrogation time [ms]	160	160	160	160	243	243	243
Source mass configurations	Fig. 2	Fig. 2	Fig. 3	Fig. 6		Fig. 5	Fig. 7
PDD [rad]	0.547870	0.530535	0.468599	0.523494		3.85769	4.72602
RSD [ppm]	148	275	75	60	10	23	17
Shift [ppm]		199	120	96		45	35
Reference	[1]				[2]		

**ders between the floors of the source mass should lead to an improvement in the accuracy of the Newton gravitational constant measurement by a factor of 3.7 [compare (eqs. 29a, 37a)].**

Following the statement [2], that 13-ton source mass can be implemented in the experiment, we increased the number of cylinders to 606 (more than 25 times). At the same time, the PDD increased only 8.4 times [compare (eq. 45) and (eq. 36)], and this increase is partly due to an increase in the delay time between the Raman pulses  $T$ . This example shows that an increase in the weight of the source mass does not even lead to a proportional signal increase. More promising here is an increase in the signal due to the larger value of the effective wave vector  $k$ , longer interrogation time  $T$ , and the optimal aspect ratio of the source mass. Due to these factors we predicted [13] PDD  $\Delta_s^{(2)}\phi = 386.527\text{rad}$  even for a source mass  $M = 1080\text{kg}$ .

We showed that for the parameters chosen for estimates in [2], our methods of dividing a source mass in 3 parts, leads to the measurement accuracy 23ppm, comparable with 10ppm accuracy predicted in [2] for an alternative method [21] of eliminating the gravity gradient tensor.

We also performed calculations for the source mass consisting of 4 quarters. In this case, in the  $F$ -configuration, the 1st and 2nd floors of the source mass can be located under the 1st AI, while the 3rd and 4th floors above the 2nd AI. As a result, the contribution to the PDD from the point of the minimum  $(z_1, v_{z1})$ , or from the point of the maximum  $(z_2, v_{z2})$  will increase leading possibly to the smaller value of RSD. If one still uses 24 cylinders, as in [1, 11], after dividing them in 4 equal quarters, the gravitational field is too weak to compensate the gradient of the Earth's field. As a re-

Another application of our formulas is the calculation of the systematic error due to the finite size of atomic clouds and their finite temperature [13, 18]. Let us now assume that  $\delta\mathbf{x}$  is the deviation of the atom from the center of the cloud and  $\delta\mathbf{v}$  is the deviation from the center of the atomic velocity distribution. If the temperatures are

sult, there are no local extremes in the  $F$ -configuration. To get extremes one needs at least 32 cylinders. It is reasonable for us to consider this situation, since even larger amount of cylinders have been used, for example, in the article [38]. We arrived to the following result (see Appendix D 1 )

$$\Delta^2\phi = 0.523511\text{rad}, \quad (49a)$$

$$\sigma\left(\delta\Delta^{(2)}\phi\right) = 60\text{ppm} \left[1 + 1.32 \cdot 10^{-15} (\Gamma_{E31}^2 + \Gamma_{E32}^2)\right]^{1/2}, \quad (49b)$$

$$s\left(\delta\Delta^{(2)}\phi\right) = 96\text{ppm}. \quad (49c)$$

Since we had to change the weight of the source mass, comparison with the results (eqs. 36, 37) is unfair.

We also considered the case of 4 quarters for 13-ton source mass (see Appendix D 2 ), and arrived to the following result

$$\Delta^2\phi = 4.72618\text{rad}, \quad (50a)$$

$$\sigma\left(\delta\Delta_s^{(2)}\phi\right) = 17\text{ppm} \left[1 + 6.54 \cdot 10^{14} (\Gamma_{E31}^2 + \Gamma_{E32}^2)\right]^{1/2}, \quad (50b)$$

$$s\left(\delta\Delta_s^{(2)}\phi\right) = 35\text{ppm}. \quad (50c)$$

Comparing this with (eqs. 45, 46) shows that using a source mass consisting of 4 quarters could increase PDD in a factor 1.22 and improve the measurement accuracy in a factor 1.35.

Results of the our study are summarized in the Table I, where the budgets obtained in Refs. [1, 2] are also included for comparison.

small enough to ignore the Doppler frequency shift, and the aperture of the optical field is large enough to assume that the areas of the Raman pulses do not depend on the position of atoms in the cloud, then the only reason for the dependence of the PDD on  $\{\delta\mathbf{x}, \delta\mathbf{v}\}$  is that the gravitational field  $\delta\mathbf{g}[\mathbf{x}(t)]$  is not the same for different atoms

in the cloud. In the given  $\frac{\pi}{2} - \pi - \frac{\pi}{2}$  AI, taking into account the phase dependence on coordinates and velocities, instead of the usual expression for the probability of excitation of atoms

$$\tilde{P}(\phi) = \frac{1}{2} [1 - \cos(\phi)], \quad (51)$$

one gets the relative population of the upper atomic sub-level averaged over coordinates and velocities,

$$P = \frac{1}{2} \left\{ 1 - \int d\vec{x}d\vec{v} f(\vec{x}, \vec{v}) \cos[\phi(\vec{x}, \vec{v})] \right\}, \quad (52)$$

where  $f(\vec{x}, \vec{v})$  is the distribution function of atoms. If the centers of the atomic cloud  $\{\vec{x}_0, \vec{v}_0\}$  are defined as

$$\{\vec{x}_0, \vec{v}_0\}^T = \int d\vec{x}d\vec{v} f(\vec{x}, \vec{v}) \{\vec{x}, \vec{v}\}^T, \quad (53)$$

then for a sufficiently small radius and a sufficiently low temperature of the atomic cloud one can use the expansion

$$\begin{aligned} \phi(\vec{x}, \vec{v}) &= \phi(\vec{x}_0, \vec{v}_0) + \partial_{\vec{x}_o} \phi(\vec{x}_0, \vec{v}_0) \delta\vec{x} + \partial_{\vec{v}_o} \phi(\vec{x}_0, \vec{v}_0) \delta\vec{v} \\ &+ \frac{1}{2} \frac{\partial^2 \phi(\vec{x}_0, \vec{v}_0)}{\partial x_{0m} \partial x_{0n}} \delta x_m \delta x_n + \frac{1}{2} \frac{\partial^2 \phi_s(\vec{x}_0, \vec{v}_0)}{\partial v_{0m} \partial v_{0n}} \delta v_m \delta v_n \\ &+ \frac{\partial^2 \phi(\vec{x}_0, \vec{v}_0)}{\partial x_{0m} \partial v_{0n}} \delta x_m \delta v_n. \end{aligned} \quad (54)$$

Due to the chosen definition of the centers (53), the linear terms in the expansion (eq. 54) can be omitted. For statistically independent distributions on coordinates and velocities, when

$$\int d\vec{x}d\vec{v} f(\vec{x}, \vec{v}) \delta x_m \delta x_n = \frac{a_m^2}{2} \delta_{mn}, \quad (55)$$

$$\int d\vec{x}d\vec{v} f(\vec{x}, \vec{v}) \delta v_m \delta v_n = \frac{\bar{v}_m^2}{2} \delta_{mn}, \quad (56)$$

$$\int d\vec{x}d\vec{v} f(\vec{x}, \vec{v}) \delta x_m \delta v_n = 0, \quad (57)$$

where  $a_m$  and  $\bar{v}_m$  are the radius and thermal velocity of the atomic cloud along the  $m$ -axis, one gets

$$\begin{aligned} P(\phi) &= \frac{1}{2} \left\{ 1 - \cos[\phi(\vec{x}_0, \vec{v}_0)] + \frac{1}{4} \sin[\phi(\vec{x}_0, \vec{v}_0)] \right. \\ &\times \left. \left( a_m^2 \frac{\partial^2 \phi(\vec{x}_0, \vec{v}_0)}{\partial x_{0m}^2} + \bar{v}_m^2 \frac{\partial^2 \phi(\vec{x}_0, \vec{v}_0)}{\partial v_{0m}^2} \right) \right\} \end{aligned} \quad (58)$$

If, despite the non-zero values of the radii and temperatures of atomic clouds, one wants to use Eq. (51) to determine the phase AI  $\bar{\phi}$ , i.e. if  $\bar{\phi}$  is the root of the equation  $\tilde{P}(\bar{\phi}) = P$ , then for  $|\bar{\phi} - \phi(\vec{x}_0, \vec{v}_0)| \ll |\bar{\phi}|$  one finds finally

$$\bar{\phi} \approx \phi(\vec{x}_0, \vec{v}_0) + \frac{1}{4} \left( a_m^2 \frac{\partial^2 \phi}{\partial x_m^2} + \bar{v}_m^2 \frac{\partial^2 \phi}{\partial v_m^2} \right). \quad (59)$$

Here we pay attention to the fact that at equal radii,  $a_x = a_y = a_z$ , and temperatures,  $v_{0x} = v_{0y} = v_{0z}$ , the systematic error in (eq. 59) disappears. This follows from the (eqs. 22c, 22e) and from the fact that the gravitational field obeys the Laplace equation and, therefore, the trace of the gravitational field curvature tensor (eq.

$$23) \sum_{m=1}^3 \chi_{s3mm} = 0.$$

## Acknowledgments

Author is appreciated to Dr. M. Prevedeli for the fruitful discussions and to Dr. G. Rosi for the explanation of some points in the article [2].

## Appendix A: Source mass consisting of 2 halves.

For the source mass and atomic fountains positioning shown in the Fig. 2, the Table II contains relative contributions to the PDD from two configurations. Besides the phase values, linear and quadratic terms in the relative phase variations, due to the uncertainties of atomic coordinates and velocities, obtained using Eqs. (11, 12, 22), are also given. Here and below we used the value of the  $zz$ -component of the gravity gradient tensor of the Earth field,

$$\Gamma_{E33} = 3.11 \cdot 10^3 \text{E}, \quad (\text{A1})$$

TABLE II: Source mass consisting of 2 halves. Relative contributions to the phase double difference (PDD) and error budget for two configurations of source mass

Term	C-configuration	F-configuration
$\phi_s^I(z_i, v_{zi})/\Delta^2\phi$	0.354, -0.330	-0.143, 0.172
Linear in position	$0.322\delta z_{1C} + 0.117\delta z_{2C} + 7.77 \cdot 10^5$ $\times [\Gamma_{E31}(\delta x_{1C} - \delta x_{2C}) + \Gamma_{E32}(\delta y_{1C} - \delta y_{2C})]$	$0.132\delta z_{1F} + 0.518\delta z_{2F} - 7.77 \cdot 10^5$ $\times [\Gamma_{E31}(\delta x_{1F} - \delta x_{2F}) + \Gamma_{E32}(\delta y_{1F} - \delta y_{2F})]$
Linear in velocity	$0.0377\delta v_{z1C} + 0.0150\delta v_{z2C} + 1.24 \cdot 10^5$ $\times [\Gamma_{E31}(\delta v_{x1C} - \delta v_{x2C}) + \Gamma_{E32}(\delta v_{y1C} - \delta v_{y2C})]$	$0.0132\delta v_{z1F} + 0.0683\delta v_{z2F} - 1.24 \cdot 10^5$ $\times [\Gamma_{E31}(\delta v_{x1F} - \delta v_{x2F}) + \Gamma_{E32}(\delta v_{y1F} - \delta v_{y2F})]$
Nonlinear in position	$12.3(\delta x_{1C}^2 + \delta y_{1C}^2) - 24.7\delta z_{1C}^2$ $+12.2(\delta x_{2C}^2 + \delta y_{2C}^2) - 24.3\delta z_{2C}^2$	$15.5(\delta x_{1F}^2 + \delta y_{1F}^2) - 30.9\delta z_{1F}^2$ $+15.7(\delta x_{2F}^2 + \delta y_{2F}^2) - 31.3\delta z_{2F}^2$
Nonlinear in velocity	$0.375(\delta v_{x1C}^2 + \delta v_{y1C}^2) - 0.750\delta v_{z1C}^2$ $+0.351(\delta v_{x2C}^2 + \delta v_{y2C}^2) - 0.702\delta v_{z2C}^2$	$0.451(\delta v_{x1F}^2 + \delta v_{y1F}^2) - 0.901\delta v_{z1F}^2$ $+0.468(\delta v_{x2F}^2 + \delta v_{y2F}^2) - 0.937\delta v_{z2F}^2$
Position-velocity cross term	$3.99(\delta v_{x1C}\delta x_{1C} + \delta v_{y1C}\delta y_{1C}) - 7.97\delta v_{z1C}\delta z_{1C}$ $+4.05(\delta v_{x2C}\delta x_{2C} + \delta v_{y2C}\delta y_{2C}) - 8.10\delta v_{z2C}\delta z_{2C}$	$5.10(\delta v_{x1F}\delta x_{1F} + \delta v_{y1F}\delta y_{1F}) - 10.2\delta v_{z1F}\delta z_{1F}$ $+5.08(\delta v_{x2F}\delta x_{2F} + \delta v_{y2F}\delta y_{2F}) - 10.2\delta v_{z2F}\delta z_{2F}$

measured in the article [39]. Using data from the Table II and (eqs. 8a, 8b, 16, 17), we obtained following error budget and shift

$$\begin{aligned}
\sigma(\Delta_s^{(2)}\phi) &= \{0.104\sigma^2(z_{1C}) + 0.0137\sigma^2(z_{2C}) + 1.42 \cdot 10^{-3}\sigma^2(v_{z1C}) + 2.24 \cdot 10^{-4}\sigma^2(v_{z2C}) \\
&+ 0.0173\sigma^2(z_{1F}) + 0.269\sigma^2(z_{2F}) + 1.75 \cdot 10^{-4}\sigma^2(v_{z1F}) + 4.66 \cdot 10^{-3}\sigma^2(v_{z2F}) \\
&+ \sum_{j=1,2} \sum_{I=C,F} [6.04 \cdot 10^{11} (\Gamma_{E31}^2\sigma^2(x_{jI}) + \Gamma_{E32}^2\sigma^2(y_{jI})) + 1.55 \cdot 10^{10} (\Gamma_{E31}^2\sigma^2(v_{xjI}) + \Gamma_{E32}^2\sigma^2(v_{yjI}))] \\
&+ 305 [\sigma^4(x_{1C}) + \sigma^4(y_{1C})] + 1220\sigma^4(z_{1C}) + 296 [\sigma^4(x_{2C}) + \sigma^4(y_{2C})] + 1180\sigma^4(z_{2C}) \\
&+ 0.282 [\sigma^4(v_{x1C}) + \sigma^4(v_{y1C})] + 1.13\sigma^4(v_{z1C}) + 0.247 [\sigma^4(v_{x2C}) + \sigma^4(v_{y2C})] + 0.987\sigma^4(v_{z2C}) \\
&+ 15.9 [\sigma^2(x_{1C})\sigma^2(v_{x1C}) + \sigma^2(y_{1C})\sigma^2(v_{y1C})] + 63.5\sigma^2(z_{1C})\sigma^2(v_{z1C}) \\
&+ 16.4 [\sigma^2(x_{2C})\sigma^2(v_{x2C}) + \sigma^2(y_{2C})\sigma^2(v_{y2C})] + 65.6\sigma^2(z_{2C})\sigma^2(v_{z2C}) \\
&+ 478 [\sigma^4(x_{1F}) + \sigma^4(y_{1F})] + 1910\sigma^4(z_{1F}) + 490 [\sigma^4(x_{2F}) + \sigma^4(y_{2F})] + 1960\sigma^4(z_{2F}) + \\
&+ 0.406 [\sigma^4(v_{x1F}) + \sigma^4(v_{y1F})] + 1.63\sigma^4(v_{z1F}) + 0.439 [\sigma^4(v_{x2F}) + \sigma^4(v_{y2F})] + 1.76\sigma^4(v_{z2F}) \\
&+ 26.0 [\sigma^2(x_{1F})\sigma^2(v_{x1F}) + \sigma^2(y_{1F})\sigma^2(v_{y1F})] + 104\sigma^2(z_{1F})\sigma^2(v_{z1F}) \\
&+ 25.8 [\sigma^2(x_{2F})\sigma^2(v_{x2F}) + \sigma^2(y_{2F})\sigma^2(v_{y2F})] + 103\sigma^2(z_{2F})\sigma^2(v_{z2F})\}^{1/2}, \tag{A2a}
\end{aligned}$$

$$\begin{aligned}
s(\Delta_s^{(2)}\phi) &= 12.3 [\sigma^2(x_{1C}) + \sigma^2(y_{1C})] - 24.7\sigma^2(z_{1C}) + 12.2 [\sigma^2(x_{2C}) + \sigma^2(y_{2C})] - 24.3\sigma^2(v_{z2C}) \\
&+ 0.375 [\sigma^2(v_{x1C}) + \sigma^2(v_{y1C})] - 0.750\sigma^2(v_{z1C}) + 0.351 [\sigma^2(v_{x2C}) + \sigma^2(v_{y2C})] - 0.702\sigma^2(v_{z2C}) \\
&+ 15.5 [\sigma^2(x_{1F}) + \sigma^2(y_{1F})] - 30.9\sigma^2(z_{1F}) + 15.7 [\sigma^2(x_{2F}) + \sigma^2(y_{2F})] - 31.3\sigma^2(z_{2F}) \\
&+ 0.451 [\sigma^2(v_{x1F}) + \sigma^2(v_{y1F})] - 0.902\sigma^2(v_{z1F}) + 0.468 [\sigma^2(v_{x2F}) + \sigma^2(v_{y2F})] - 0.937\sigma^2(v_{z2F}). \tag{A2b}
\end{aligned}$$

### Appendix B: Source mass consisting of 3 parts.

For the source mass and atomic fountains positioning shown in the Fig. 3, using (eq. A1) we arrived to the relative contributions to the PDD listed in the Table III. One sees that despite the choice of extreme points, linear dependences on  $\{\delta z_{jI}, \delta v_{zjI}\}$  in the phase variation do not completely disappear. This is because extrema (eq. 31) and positions of the source mass parts in the  $F$ -configuration (eq. 34) were found approximately. Here and below negligible linear terms will be excluded from the calculation. Using data from this table and (eqs. 8a, 8b, 16, 17), we

TABLE III: The same as in Table II but for the source mass concicting of 3 parts

Term	C-configuration	F-configuration
$\phi_s^I(z_i, v_{zi})/\Delta^2\phi$	0.309, -0.321	-0.140, 0.230
Linear in position	$10^{-7}(-1.52\delta z_{1C} + 1.28\delta z_{2C}) + 8.80 \cdot 10^9$ $\times [\Gamma_{E31}(\delta x_{1C} - \delta x_{2C}) + \Gamma_{E32}(\delta y_{1C} - \delta y_{2C})]$	$10^{-8}(1.29\delta z_{1F} + 3.57\delta z_{2F}) - 8.80 \cdot 10^9$ $\times [\Gamma_{E31}(\delta x_{1F} - \delta x_{2F}) + \Gamma_{E32}(\delta y_{1F} - \delta y_{2F})]$
Linear in velocity	$10^{-8}(-3.38\delta v_{z1C} + 2.18\delta v_{z2C}) + 1.41 \cdot 10^9$ $\times [\Gamma_{E31}(\delta v_{x1C} - \delta v_{x2C}) + \Gamma_{E32}(\delta v_{y1C} - \delta v_{y2C})]$	$10^{-9}(-2.97\delta v_{z1F} - 5.26\delta v_{z2F}) - 1.41 \cdot 10^9$ $\times [\Gamma_{E31}(\delta v_{x1F} - \delta v_{x2F}) + \Gamma_{E32}(\delta v_{y1F} - \delta v_{y2F})]$
Nonlinear in position	$3.36\delta x_{1C}^2 + 6.22\delta y_{1C}^2 - 9.58\delta z_{1C}^2$ $+ 5.00\delta x_{2C}^2 + 8.07\delta y_{2C}^2 - 13.1\delta z_{2C}^2$	$13.3\delta x_{1F}^2 + 16.2\delta y_{1F}^2 - 29.5\delta z_{1F}^2$ $+ 6.26\delta x_{2F}^2 + 9.15\delta y_{2F}^2 - 15.4\delta z_{2F}^2$
Nonlinear in velocity	$0.126\delta v_{x1C}^2 + 0.215\delta v_{y1C}^2 - 0.341\delta v_{z1C}^2$ $+ 0.117\delta v_{x2C}^2 + 0.203\delta v_{y2C}^2 - 0.320\delta v_{z2C}^2$	$0.362\delta v_{x1F}^2 + 0.443\delta v_{y1F}^2 - 0.805\delta v_{z1F}^2$ $+ 0.207\delta v_{x2F}^2 + 0.297\delta v_{y2F}^2 - 0.504319\delta v_{z2F}^2$
Position-velocity cross term	$1.07\delta v_{x1C}\delta x_{1C} + 1.99\delta v_{y1C}\delta y_{1C} - 3.06\delta v_{z1C}\delta z_{1C}$ $+ 1.60\delta v_{x2C}\delta x_{2C} + 2.58\delta v_{y2C}\delta y_{2C} - 4.18\delta v_{z2C}\delta z_{2C}$	$4.24\delta v_{x1F}\delta x_{1F} + 5.19\delta v_{y1F}\delta y_{1F} - 9.43\delta v_{z1F}\delta z_{1F}$ $+ 2.00\delta v_{x2F}\delta x_{2F} + 2.93\delta v_{y2F}\delta y_{2F} - 4.93\delta v_{z2F}\delta z_{2F}$

obtained following error budget and shift

$$\begin{aligned}
\sigma\left(\Delta_s^{(2)}\phi\right) &= \left\{10^{10} \sum_{j=1,2} \sum_{I=C,F} [77.4(\Gamma_{E31}^2\sigma^2(x_{jI}) + \Gamma_{E32}^2\sigma^2(y_{jI})) + 1.98(\Gamma_{E31}^2\sigma^2(v_{xjI}) + \Gamma_{E32}^2\sigma^2(v_{yjI}))]\right. \\
&\quad + 22.5\sigma^4(x_{1C}) + 77.4\sigma^4(y_{1C}) + 183\sigma^4(z_{1C}) + 49.9\sigma^4(x_{2C}) + 130\sigma^4(y_{2C}) + 341\sigma^4(z_{2C}) + \\
&\quad + 0.0316\sigma^4(v_{x1C}) + 0.0926\sigma^4(v_{y1C}) + 0.232\sigma^4(v_{z1C}) + 0.0275\sigma^4(v_{x2C}) + 0.0825\sigma^4(v_{y2C}) + 0.205\sigma^4(v_{z2C}) \\
&\quad + 1.15\sigma^2(x_{1C})\sigma^2(v_{x1C}) + 3.96\sigma^2(y_{1C})\sigma^2(v_{y1C}) + 9.39\sigma^2(z_{1C})\sigma^2(v_{z1C}) \\
&\quad + 2.56\sigma^2(x_{2C})\sigma^2(v_{x2C}) + 6.66\sigma^2(y_{2C})\sigma^2(v_{y2C}) + 17.5\sigma^2(z_{2C})\sigma^2(v_{z2C}) + \\
&\quad + 352\sigma^4(x_{1F}) + 525\sigma^4(y_{1F}) + 1740\sigma^4(z_{1F}) + 78.3\sigma^4(x_{2F}) + 1685\sigma^4(y_{2F}) + 475\sigma^4(z_{2F}) \\
&\quad + 0.262\sigma^4(v_{x1F}) + 0.392\sigma^4(v_{y1F}) + 1.30\sigma^4(v_{z1F}) + 0.0858\sigma^4(v_{x2F}) + 0.177\sigma^4(v_{y2F}) + 0.509\sigma^4(v_{z2F}) \\
&\quad + 18.0\sigma^2(x_{1F})\sigma^2(v_{x1F}) + 26.9\sigma^2(y_{1F})\sigma^2(v_{y1F}) + 88.9\sigma^2(z_{1F})\sigma^2(v_{z1F}) \\
&\quad \left. + 4.01\sigma^2(x_{2F})\sigma^2(v_{x2F}) + 8.58\sigma^2(y_{2F})\sigma^2(v_{y2F}) + 24.3\sigma^2(z_{2F})\sigma^2(v_{z2F})\right\}^{1/2} \quad (\text{B3a}) \\
s\left(\Delta_s^{(2)}\phi\right) &= 3.36\sigma^2(x_{1C}) + 6.22\sigma^2(y_{1C}) - 9.58\sigma^2(z_{1C}) + 5.00\sigma^2(x_{2C}) + 8.07\sigma^2(y_{2C}) - 13.1\sigma^2(z_{2C}) \\
&\quad + 0.126\sigma^2(v_{x1C}) + 0.215\sigma^2(v_{y1C}) - 0.341\sigma^2(v_{z1C}) + 0.117\sigma^2(v_{x2C}) + 0.203\sigma^2(v_{y2C}) - 0.320\sigma^2(v_{z2C}) \\
&\quad + 13.3\sigma^2(x_{1F}) + 16.2\sigma^2(y_{1F}) - 29.5\sigma^2(z_{1F}) + 6.26\sigma^2(x_{2F}) + 9.15\sigma^2(y_{2F}) - 15.4\sigma^2(z_{2F}) \\
&\quad + 0.362\sigma^2(v_{x1F}) + 0.443\sigma^2(v_{y1F}) - 0.805\sigma^2(v_{z1F}) + 0.207\sigma^2(v_{x2F}) + 0.297\sigma^2(v_{y2F}) - 0.504\sigma^2(v_{z2F}). \quad (\text{B3b})
\end{aligned}$$

### Appendix C: 13-ton source mass.

For the source mass and atomic fountains positioning shown in the Fig. 5, using (eq. A1) we arrived to the relative contributions to the PDD listed in the Table IV. Using data from this table and (eqs. 8a, 8b, 16, 17), we obtained

TABLE IV: The same as in Table II but for the 13 tons source mass.

Term	C-configuration	F-configuration
$\phi'_s(z_i, v_{zi})/\Delta^2\phi$	0.418, -0.398	-0.188, $-3.90 \cdot 10^{-3}$
Linear in position	$10^{-10}(-11.0\delta z_{1C} + 8.63\delta z_{2C}) + 2.47 \cdot 10^5$ $\times [\Gamma_{E31}(\delta x_{1C} - \delta x_{2C}) + \Gamma_{E32}(\delta y_{1C} - \delta y_{2C})]$	$10^{-9}(-7.36\delta z_{1F} - 10.8\delta z_{2F}) - 2.47 \cdot 10^5$ $\times [\Gamma_{E31}(\delta x_{1F} - \delta x_{2F}) + \Gamma_{E32}(\delta y_{1F} - \delta y_{2F})]$
Linear in velocity	$10^{-10}(-2.97\delta v_{z1C} + 2.09\delta v_{z2C}) + 5.99 \cdot 10^4$ $\times [\Gamma_{E31}(\delta v_{x1C} - \delta v_{x2C}) + \Gamma_{E32}(\delta v_{y1C} - \delta v_{y2C})]$	$10^{-9}(-1.79\delta v_{z1F} - 2.25\delta v_{z2F}) - 5.99 \cdot 10^4$ $\times [\Gamma_{E31}(\delta v_{x1F} - \delta v_{x2F}) + \Gamma_{E32}(\delta v_{y1F} - \delta v_{y2F})]$
Nonlinear in position	$4.61(\delta x_{1C}^2 + \delta y_{1C}^2) - 9.22\delta z_{1C}^2$ $+4.29\delta x_{2C}^2 + 4.30\delta y_{2C}^2 - 8.59\delta z_{2C}^2$	$4.24[\delta x_{1F}^2 + \delta y_{1F}^2] - 8.47\delta z_{1F}^2$ $+5.10[\delta x_{2F}^2 + \delta y_{2F}^2] - 10.2\delta z_{2F}^2$
Nonlinear in velocity	$0.297(\delta v_{x1C}^2 + \delta v_{y1C}^2) - 0.594\delta v_{z1C}^2$ $+0.270(\delta v_{x2C}^2 + \delta v_{y2C}^2) - 0.540\delta v_{z2C}^2$	$0.264[\delta v_{x1F}^2 + \delta v_{y1F}^2] - 0.527\delta v_{z1F}^2$ $+0.326[\delta v_{x2F}^2 + \delta v_{y2F}^2] - 0.652\delta v_{z2F}^2$
Position-velocity cross term	$2.24(\delta v_{x1C}\delta x_{1C} + \delta v_{y1C}\delta y_{1C}) - 4.48\delta v_{z1C}\delta z_{1C}$ $+2.09(\delta v_{x2C}\delta x_{2C} + \delta v_{y2C}\delta y_{2C}) - 4.18\delta v_{z2C}\delta z_{2C}$	$2.06[\delta v_{x1F}\delta x_{1F} + \delta v_{y1F}\delta y_{1F}] - 4.12\delta v_{z1F}\delta z_{1F}$ $+2.48[\delta v_{x2F}\delta x_{2F} + \delta v_{y2F}\delta y_{2F}] - 4.96\delta v_{z2F}\delta z_{2F}$

following error budget and shift

$$\begin{aligned} \sigma(\Delta_s^{(2)}\phi) = & \left\{ 10^9 \sum_{j=1,2} \sum_{I=C,F} [60.8(\Gamma_{E31}^2\sigma^2(x_{jI}) + \Gamma_{E32}^2\sigma^2(y_{jI})) + 3.59(\Gamma_{E31}^2\sigma^2(v_{xjI}) + \Gamma_{E32}^2\sigma^2(v_{yjI}))] \right. \\ & + 42.4\sigma^4(x_{1C}) + 42.6\sigma^4(y_{1C}) + 170\sigma^4(z_{1C}) + 36.9\sigma^4(x_{2C}) + 37.0\sigma^4(y_{2C}) + 148\sigma^4(z_{2C}) + \\ & + 0.176\sigma^4(v_{x1C}) + 0.177\sigma^4(v_{y1C}) + 0.706\sigma^4(v_{z1C}) + 0.146[\sigma^4(v_{x2C}) + \sigma^4(v_{y2C})] + 0.583\sigma^4(v_{z2C}) \\ & + 5.01\sigma^2(x_{1C})\sigma^2(v_{x1C}) + 5.03\sigma^2(y_{1C})\sigma^2(v_{y1C}) + 20.1\sigma^2(z_{1C})\sigma^2(v_{z1C}) \\ & + 4.36\sigma^2(x_{2C})\sigma^2(v_{x2C}) + 4.37\sigma^2(y_{2C})\sigma^2(v_{y2C}) + 17.4\sigma^2(z_{2C})\sigma^2(v_{z2C}) + \\ & + 35.9[\sigma^4(x_{1F}) + \sigma^4(y_{1F})] + 144\sigma^4(z_{1F}) + 52.1\sigma^4(x_{2F}) + 52.0\sigma^4(y_{2F}) + 208\sigma^4(z_{2F}) \\ & + 0.139[\sigma^4(v_{x1F}) + \sigma^4(v_{y1F})] + 0.556\sigma^4(v_{z1F}) + 0.213\sigma^4(v_{x2F}) + 0.212\sigma^4(v_{y2F}) + 0.850\sigma^4(v_{z2F}) \\ & + 4.24[\sigma^2(x_{1F})\sigma^2(v_{x1F}) + \sigma^2(y_{1F})\sigma^2(v_{y1F})] + 17.0\sigma^2(z_{1F})\sigma^2(v_{z1F}) \\ & \left. + 6.15[\sigma^2(x_{2F})\sigma^2(v_{x2F}) + \sigma^2(y_{2F})\sigma^2(v_{y2F})] + 24.6\sigma^2(z_{2F})\sigma^2(v_{z2F})\right\}^{1/2}, \end{aligned} \quad (C4a)$$

$$\begin{aligned} s(\Delta_s^{(2)}\phi) = & 4.61[\sigma^2(x_{1C}) + \sigma^2(y_{1C})] - 9.22\sigma^2(z_{1C}) + 4.29\sigma^2(x_{2C}) + 4.30\sigma^2(y_{2C}) - 8.59\sigma^2(z_{2C}) \\ & + 0.297[\sigma^2(v_{x1C}) + \sigma^2(v_{y1C})] - 0.594\sigma^2(v_{z1C}) + 0.270[\sigma^2(v_{x2C}) + \sigma^2(v_{y2C})] - 0.540\sigma^2(v_{z2C}) \\ & + 4.24[\sigma^2(x_{1F}) + \sigma^2(y_{1F})] - 8.47\sigma^2(z_{1F}) + 5.10[\sigma^2(x_{2F}) + \sigma^2(y_{2F})] - 10.2\sigma^2(z_{2F}) \\ & + 0.264[\sigma^2(v_{x1F}) + \sigma^2(v_{y1F})] - 0.527\sigma^2(v_{z1F}) + 0.326[\sigma^2(v_{x2F}) + \sigma^2(v_{y2F})] - 0.652\sigma^2(v_{z2F}). \end{aligned} \quad (C4b)$$

## Appendix D: Source mass consisting of 4 quarters

### 1. Minimal source mass

We performed calculations for the source mass geometry shown in Fig. 6.

This is a minimal amount of cylinders used in [1], when 4 quarters of the source mass produce a sufficiently strong gravitational field to make all atomic variables extreme in the both configurations. Instead of Eqs. (31, 32, 34-36) we arrived to the following results

$$z_1 = -0.0550\text{m}, z_2 = 0.599\text{m}, v_{z1} = v_{z2} = v = 1.563\text{m/s}, \quad (D5a)$$

$$\{\phi_s^{(C)}(z_1, v), \phi_s^{(C)}(z_2, v)\} = \{0.150759\text{rad}, -0.157911\text{rad}\}, \quad (D5b)$$

$$\{h_1, h_2, h_3, h_4\} = \{-0.277\text{m}, -0.0632\text{m}, 0.681\text{m}, 1.10\text{m}\}, \quad (D5c)$$

$$\{\phi_s^{(F)}(z_1, v), \phi_s^{(F)}(z_2, v)\} = \{-0.118580\text{rad}, 0.096261\text{rad}\}, \quad (D5d)$$

$$\Delta^2\phi = 0.523511\text{rad}. \quad (D5e)$$

Relative contributions to the PDD listed now in the Table V. Using data from this table and (eqs. 8a, 8b, 16, 17),

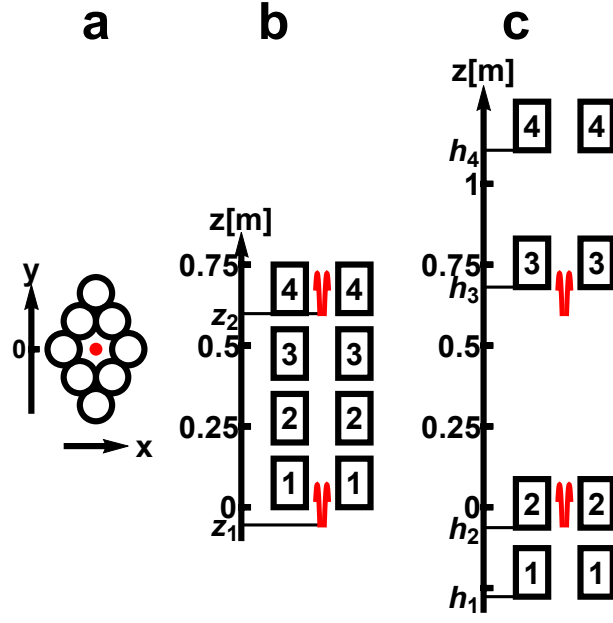


FIG. 6: The same as Fig. 3 but for the source mass consisting of 4 quarters.

TABLE V: The same as in Table II but for the source mass geometry shown in Fig. 6.

Term	C-configuration	F-configuration
$\phi_s^I(z_i, v_{zi})/\Delta^2\phi$	0.288, -0.302	-0.227, 0.184
Linear in position	$10^{-8} (3.79\delta z_{1C} - 139.\delta z_{2C}) + 7.88 \cdot 10^5 \cdot$ $\times [\Gamma_{E31} (\delta x_{1C} - \delta x_{2C}) + \Gamma_{E32} (\delta y_{1C} - \delta y_{2C})]$	$10^{-7} (-2.45\delta z_{1F} - 27.3\delta z_{2F}) - 7.88 \cdot 10^5 \cdot$ $\times [\Gamma_{E31} (\delta x_{1F} - \delta x_{2F}) + \Gamma_{E32} (\delta y_{1F} - \delta y_{2F})]$
Linear in velocity	$10^{-9} (6.92\delta v_{z1C} - 296\delta v_{z2C}) + 1.26 \cdot 10^9 \cdot$ $\times [\Gamma_{E31} (\delta v_{x1C} - \delta v_{x2C}) + \Gamma_{E32} (\delta v_{y1C} - \delta v_{y2C})]$	$10^{-8} (-3.91\delta v_{z1F} - 4.52\delta v_{z2F}) - 1.26 \cdot 10^9 \cdot$ $\times [\Gamma_{E31} (\delta v_{x1F} - \delta v_{x2F}) + \Gamma_{E32} (\delta v_{y1F} - \delta v_{y2F})]$
Nonlinear in position	$2.14\delta x_{1C}^2 + 4.53\delta y_{1C}^2 - 6.67\delta z_{1C}^2$ $+ 3.48\delta x_{2C}^2 + 6.12\delta y_{2C}^2 - 9.60\delta z_{2C}^2$	$7.03\delta x_{1F}^2 + 9.83\delta y_{1F}^2 - 16.9\delta z_{1F}^2$ $+ 9.17\delta x_{2F}^2 + 11.9\delta y_{2F}^2 - 21.0\delta z_{2F}^2$
Nonlinear in velocity	$0.0879\delta v_{x1C}^2 + 0.163\delta v_{y1C}^2 - 0.251\delta v_{z1C}^2$ $+ 0.0762\delta v_{x2C}^2 + 0.150\delta v_{y2C}^2 - 0.226\delta v_{z2C}^2$	$0.179\delta v_{x1F}^2 + 0.257\delta v_{y1F}^2 - 0.437\delta v_{z1F}^2$ $+ 0.281\delta v_{x2F}^2 + 0.364\delta v_{y2F}^2 - 0.644\delta v_{z2F}^2$
Position-velocity cross term	$0.685\delta v_{x1C}\delta x_{1C} + 1.45\delta v_{y1C}\delta y_{1C} - 2.14\delta v_{z1C}\delta z_{1C}$ $+ 1.11\delta v_{x2C}\delta x_{2C} + 1.96\delta v_{y2C}\delta y_{2C} - 3.07\delta v_{z2C}\delta z_{2C}$	$2.25\delta v_{x1F}\delta x_{1F} + 3.15\delta v_{y1F}\delta y_{1F} - 5.40\delta v_{z1F}\delta z_{1F}$ $+ 2.93\delta v_{x2F}\delta x_{2F} + 3.80\delta v_{y2F}\delta y_{2F} - 6.73\delta v_{z2F}\delta z_{2F}$

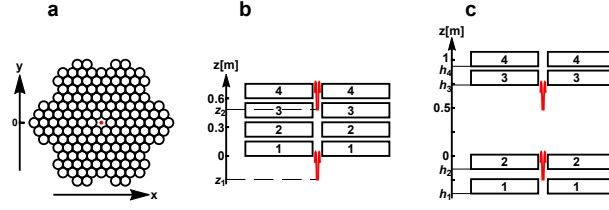


FIG. 7: The same as Fig. 5 but for the source mass consisting of 4 quarters

we obtained following error budget and shift

$$\begin{aligned} \sigma \left( \Delta_s^{(2)} \phi \right) = & \left\{ 10^{10} \sum_{j=1,2} \sum_{I=C,F} [62.0 (\Gamma_{E31}^2 \sigma^2 (x_{jI}) + \Gamma_{E32}^2 \sigma^2 (y_{jI})) + 1.59 (\Gamma_{E31}^2 \sigma^2 (v_{xjI}) + \Gamma_{E32}^2 \sigma^2 (v_{yjI}))] \right. \\ & + 9.16\sigma^4 (x_{1C}) + 41.1\sigma^4 (y_{1C}) + 89.1\sigma^4 (z_{1C}) + 24.2\sigma^4 (x_{2C}) + 74.8\sigma^4 y_{2C} + 184\sigma^4 (z_{2C}) \\ & + 0.0155\sigma^4 (v_{x1C}) + 0.0534\sigma^4 (v_{y1C}) + 0.126\sigma^4 (v_{z1C}) + 0.0116\sigma^4 (v_{x2C}) + 0.0449\sigma^4 (v_{y2C}) + 0.102\sigma^4 (v_{z2C}) \\ & + 0.469\sigma^2 (x_{1C}) \sigma^2 (v_{x1C}) + 2.11\sigma^2 (y_{1C}) \sigma^2 (v_{y1C}) + 4.56\sigma^2 (z_{1C}) \sigma^2 (v_{z1C}) \\ & + 1.24\sigma^2 (x_{2C}) \sigma^2 (v_{x2C}) + 3.83\sigma^2 (y_{2C}) \sigma^2 (v_{y2C}) + 9.43\sigma^2 (z_{2C}) \sigma^2 (v_{z2C}) \\ & + 98.9\sigma^4 (x_{1F}) + 193\sigma^4 (y_{1F}) + 569\sigma^4 (z_{1F}) + 168\sigma^4 (x_{2F}) + 282\sigma^4 (y_{2F}) + 885\sigma^4 (z_{2F}) + \\ & + 0.0643\sigma^4 (v_{x1F}) + 0.132\sigma^4 (v_{y1F}) + 0.381\sigma^4 (v_{z1F}) + 0.157\sigma^4 (v_{x2F}) + 0.265\sigma^4 (v_{y2F}) + 0.830\sigma^4 (v_{z2F}) \\ & + 5.06\sigma^2 (x_{1F}) \sigma^2 (v_{x1F}) + 9.90\sigma^2 (y_{1F}) \sigma^2 (v_{y1F}) + 29.1\sigma^2 (z_{1F}) \sigma^2 (v_{z1F}) \\ & \left. + 8.60\sigma^2 (x_{2F}) \sigma^2 (v_{x2F}) + 14.4\sigma^2 (y_{2F}) \sigma^2 (v_{y2F}) + 45.3\sigma^2 (z_{2F}) \sigma^2 (v_{z2F}) \right\}^{1/2}, \end{aligned} \quad (D6a)$$

$$\begin{aligned} s \left( \Delta_s^{(2)} \phi \right) = & 2.14\sigma^2 (x_{1C}) + 4.53\sigma^2 (y_{1C}) - 6.67\sigma^2 (z_{1C}) + 3.48\sigma^2 (x_{2C}) + 6.12\sigma^2 (y_{2C}) - 9.60\sigma^2 (z_{2C}) \\ & + 0.0879\sigma^2 (v_{x1C}) + 0.163\sigma^2 (v_{y1C}) - 0.251\sigma^2 (v_{z1C}) + 0.0762\sigma^2 (v_{x2C}) + 0.150\sigma^2 (v_{y2C}) - 0.226\sigma^2 (v_{z2C}) \\ & + 7.03\sigma^2 (x_{1F}) + 9.83\sigma^2 (y_{1F}) - 16.9\sigma^2 (z_{1F}) + 9.17\sigma^2 (x_{2F}) + 11.9\sigma^2 (y_{2F}) - 21.0\sigma^2 (z_{2F}) \\ & + 0.179\sigma^2 (v_{x1F}) + 0.257\sigma^2 (v_{y1F}) - 0.437\sigma^2 (v_{z1F}) + 0.281\sigma^2 (v_{x2F}) + 0.364\sigma^2 (v_{y2F}) - 0.644\sigma^2 (v_{z2F}). \end{aligned} \quad (D6b)$$

Substituting here uncertainties of the atomic variables (eq. 28) one gets instead of (eqs. 37, 38)

$$\sigma \left( \delta \Delta^{(2)} \phi \right) = 60\text{ppm} [1 + 1.32 \cdot 10^{15} (\Gamma_{E31}^2 + \Gamma_{E32}^2)]^{1/2}, \quad (D7a)$$

$$s \left( \delta \Delta^{(2)} \phi \right) = 96\text{ppm}, \quad (D7b)$$

$$\sqrt{\Gamma_{E31}^2 + \Gamma_{E32}^2} < 6E. \quad (D7c)$$

## 2. 13-ton source mass

A symmetric in the horizontal plane source mass, which can be divided in 4 quarters and has a minimal total weight exceeding 13 tons, is shown in the fig. 7

Instead of (eqs. 41 - 45) we arrived to the following results

$$z_1 = -0.244\text{m}, z_2 = 0.483\text{m}, v_{z1} = v_{z2} = v = 2.377\text{m/s}, \quad (D8a)$$

$$\left\{ \phi_s^{(C)}(z_1, v), \phi_s^{(C)}(z_2, v) \right\} = \{1.73227\text{rad}, -1.67980\text{rad}\}, \quad (D8b)$$

$$\{h_1, h_2, h_3, h_4\} = \{-0.391\text{m}, -0.136\text{m}, 0.738\text{m}, 0.933\text{m}\}, \quad (D8c)$$

$$\left\{ \phi_s^{(F)}(z_1, v), \phi_s^{(F)}(z_2, v) \right\} = \{-0.58469\text{rad}, 0.72938\text{rad}\}, \quad (D8d)$$

$$\Delta^2 \phi = 4.72618\text{rad}. \quad (D8e)$$

Relative contributions to the PDD listed now in the Table VI. Using data from this table and (eqs. 8a, 8b, 16, 17),

TABLE VI: The same as in Table II but for the source mass geometry shown in Fig. 7.

Term	C-configuration	F-configuration
$\phi_s^I(z_i, v_{zi})/\Delta^2\phi$	0.367, -0.355	-0.124, 0.154
Linear in position	$10^{-11} (3.88\delta z_{1C} - 16.5\delta z_{2C}) + 2.01 \cdot 10^9 \cdot$ $\times [\Gamma_{E31}(\delta x_{1C} - \delta x_{2C}) + \Gamma_{E32}(\delta y_{1C} - \delta y_{2C})]$	$10^{-9} [-6.50\delta z_{1F} - 7.40\delta z_{2F}] - 2.01 \cdot 10^9$ $\times [\Gamma_{E31}(\delta x_{1F} - \delta x_{2F}) + \Gamma_{E32}(\delta y_{1F} - \delta y_{2F})]$
Linear in velocity	$10^{-12} (9.49\delta v_{z1C} - 28.3\delta v_{z2C}) + 4.89 \cdot 10^4$ $\times [\Gamma_{E31}(\delta v_{x1C} - \delta v_{x2C}) + \Gamma_{E32}(\delta v_{y1C} - \delta v_{y2C})]$	$10^{-9} [-1.58\delta v_{z1F} - 1.76\delta v_{z2F}] - 4.89 \cdot 10^4$ $\times [\Gamma_{E31}(\delta v_{x1F} - \delta v_{x2F}) + \Gamma_{E32}(\delta v_{y1F} - \delta v_{y2F})]$
Nonlinear in position	$3.22\delta x_{1C}^2 + 3.21\delta y_{1C}^2 - 6.43\delta z_{1C}^2$ $+ 3.62\delta x_{2C}^2 + 3.61\delta y_{2C}^2 - 7.24\delta z_{2C}^2$	$3.45(\delta x_{1F}^2 + \delta y_{1F}^2) - 6.90\delta z_{1F}^2$ $+ 3.80(\delta x_{2F}^2 + \delta y_{2F}^2) - 7.60\delta z_{2F}^2$
Nonlinear in velocity	$0.212\delta v_{x1C}^2 + 0.211\delta v_{y1C}^2 - 0.423\delta v_{z1C}^2$ $+ 0.223(\delta v_{x2C}^2 + \delta v_{y2C}^2) - 0.446\delta v_{z2C}^2$	$0.209(\delta v_{x1F}^2 + \delta v_{y1F}^2) - 0.418\delta v_{z1F}^2$ $+ 0.246(\delta v_{x2F}^2 + \delta v_{y2F}^2) - 0.492\delta v_{z2F}^2$
Position-velocity cross term	$1.56(\delta v_{x1C}\delta x_{1C} + \delta v_{y1C}\delta y_{1C}) - 3.12\delta v_{z1C}\delta z_{1C}$ $+ 1.76(\delta v_{x2C}\delta x_{2C} + \delta v_{y2C}\delta y_{2C}) - 3.52\delta v_{z2C}\delta z_{2C}$	$1.68(\delta v_{x1F}\delta x_{1F} + \delta v_{y1F}\delta y_{1F}) - 3.35\delta v_{z1F}\delta z_{1F}$ $+ 1.85(\delta v_{x2F}\delta x_{2F} + \delta v_{y2F}\delta y_{2F}) - 3.69\delta v_{z2F}\delta z_{2F}$

we obtained following error budget and shift

$$\sigma(\Delta_s^{(2)}\phi) = \left\{ 10^9 \sum_{j=1,2} \sum_{I=C,F} [40.5(\Gamma_{E31}^2\sigma^2(x_{jI}) + \Gamma_{E32}^2\sigma^2(y_{jI})) + 2.39(\Gamma_{E31}^2\sigma^2(v_{xjI}) + \Gamma_{E32}^2\sigma^2(v_{yjI}))] \right.$$

$$+ 20.7\sigma^4(x_{1C}) + 20.6\sigma^4(y_{1C}) + 82.6\sigma^4(z_{1C}) + 26.3\sigma^4(x_{2C}) + 26.1\sigma^4(y_{2C}) + 105\sigma^4(z_{2C})$$

$$+ 0.0896\sigma^4(v_{x1C}) + 0.0889\sigma^4(v_{y1C}) + 0.357\sigma^4(v_{z1C}) + 0.0998\sigma^4(v_{x2C}) + 0.0991\sigma^4(v_{y2C}) + 0.398\sigma^4(v_{z2C})$$

$$+ 2.45\sigma^2(x_{1C})\sigma^2(v_{x1C}) + 2.43\sigma^2(y_{1C})\sigma^2(v_{y1C}) + 9.75\sigma^2(z_{1C})\sigma^2(v_{z1C})$$

$$+ 3.10\sigma^2(x_{2C})\sigma^2(v_{x2C}) + 3.08\sigma^2(y_{2C})\sigma^2(v_{y2C}) + 12.4\sigma^2(z_{2C})\sigma^2(v_{z2C})$$

$$+ 23.8[\sigma^4(x_{1F}) + \sigma^4(y_{1F})] + 95.2\sigma^4(z_{1F}) + 28.9[\sigma^4(x_{2F}) + \sigma^4(y_{2F})] + 116\sigma^4(z_{2F}) +$$

$$+ 0.0874\sigma^4(v_{x1F}) + 0.0872\sigma^4(v_{y1F}) + 0.349\sigma^4(v_{z1F}) + 0.121[\sigma^4(v_{x2F}) + \sigma^4(v_{y2F})] + 0.485\sigma^4(v_{z2F})$$

$$+ 2.81[\sigma^2(x_{1F})\sigma^2(v_{x1F}) + \sigma^2(y_{1F})\sigma^2(v_{y1F})] + 11.2\sigma^2(z_{1F})\sigma^2(v_{z1F})$$

$$+ 3.42\sigma^2(x_{2F})\sigma^2(v_{x2F}) + 3.41\sigma^2(y_{2F})\sigma^2(v_{y2F}) + 13.7\sigma^2(z_{2F})\sigma^2(v_{z2F}) \Big\}^{1/2}, \quad (\text{D9a})$$

$$s(\Delta_s^{(2)}\phi) = 3.22\sigma^2(x_{1C}) + 3.21\sigma^2(y_{1C}) - 6.43\sigma^2(z_{1C}) + 3.62\sigma^2(x_{2C}) + 3.61\sigma^2(y_{2C}) - 7.24\sigma^2(v_{z2C})$$

$$+ 0.212\sigma^2(v_{x1C}) + 0.211\sigma^2(v_{y1C}) - 0.423\sigma^2(v_{z1C}) + 0.223[\sigma^2(v_{x2C}) + \sigma^2(v_{y2C})] - 0.446\sigma^2(v_{z2C})$$

$$+ 3.45[\sigma^2(x_{1F}) + \sigma^2(y_{1F})] - 6.90\sigma^2(z_{1F}) + 3.80[\sigma^2(x_{2F}) + \sigma^2(y_{2F})] - 7.60\sigma^2(z_{2F})$$

$$+ 0.209[\sigma^2(v_{x1F}) + \sigma^2(v_{y1F})] - 0.418\sigma^2(v_{z1F}) + 0.246[\sigma^2(v_{x2F}) + \sigma^2(v_{y2F})] - 0.492\sigma^2(v_{z2F}). \quad (\text{D9b})$$

Substituting here uncertainties of the atomic variables (eqs. 28a, 28b, 40) one gets instead of (eqs. 46, 47)

$$\sigma(\delta\Delta_s^{(2)}\phi) = 17\text{ppm} [1 + 6.54 \cdot 10^{14} (\Gamma_{E31}^2 + \Gamma_{E32}^2)]^{1/2}, \quad (\text{D10a})$$

$$s(\delta\Delta_s^{(2)}\phi) = 35\text{ppm}, \quad (\text{D10b})$$

$$\sqrt{\Gamma_{E31}^2 + \Gamma_{E32}^2} < 18\text{E}. \quad (\text{D10c})$$

## Appendix E: Gravity field of the homogeneous cylinder

### 1. Axial component

It is convenient [23] to explore the following expression for the potential of the gravitational field of a homogeneous cylinder  $\Phi(\mathbf{x})$

$$\Phi(r, z) = -2G\rho \int_0^R dy \int_{r-\sqrt{R^2-y^2}}^{r+\sqrt{R^2-y^2}} d\xi \int_{z-h}^z \frac{d\zeta}{\sqrt{y^2 + \xi^2 + \zeta^2}}, \quad (\text{E11})$$

where  $\rho$ ,  $R$ , and  $h$  are the density, radius, and height of the cylinder,  $(r, z, \psi = 0)$  are the cylindrical coordinates of the vector  $\mathbf{x}$ . For an axial component of the gravitational field,  $\delta g_3(r, z) = -\partial_z \Phi(r, z)$ , one gets

$$\delta g_3(r, z) = 2G\rho g_3(r, \zeta) \Big|_{\zeta=z-h}, \quad (\text{E12})$$

where the function

$$g_3(r, \zeta) = \int_0^R dy \int_{r-\sqrt{R^2-y^2}}^{r+\sqrt{R^2-y^2}} \frac{d\xi}{\sqrt{y^2 + \xi^2 + \zeta^2}} \quad (\text{E13})$$

can be represented as

$$\begin{aligned} g_3(r, \zeta) &= \int_0^R dy \ln \frac{t_+(y)}{t_-(y)} \\ &= - \int_0^R y \left( \frac{dt_+}{t_+} - \frac{dt_-}{t_-} \right), \end{aligned} \quad (\text{E14a})$$

$$t_{\pm}(y) = r \pm \sqrt{R^2 - y^2} + \left( \zeta^2 + r^2 + R^2 \pm 2r\sqrt{R^2 - y^2} \right)^{1/2} \quad (\text{E14b})$$

Since  $t_+(R) = t_-(R) \equiv t(R) \leq t_{\pm}(0)$  one can write

$$g_3(r, \zeta) = \int_{t(R)}^{t_+(0)} \frac{dt}{t} y_+(t) + \int_{t_-(0)}^{t(R)} \frac{dt}{t} y_-(t), \quad (\text{E15})$$

where  $y_{\pm}(t)$  is the root of the equation  $t_{\pm}(y) = t$ . To find this root, consider the functions  $x_{\pm}(t) = \sqrt{R^2 - y_{\pm}^2(t)}$ ,

$$0 < x_{\pm}(t) < R. \quad (\text{E16})$$

For them one gets

$$x_{\pm}(t) = \pm t + \sqrt{\zeta^2 + R^2 + 2tr} \text{ or } \pm t - \sqrt{\zeta^2 + R^2 + 2tr} \quad (\text{E17})$$

Since  $t + \sqrt{\zeta^2 + R^2 + 2tr} > R$ , then one should choose  $x_+(t) = t - \sqrt{\zeta^2 + R^2 + 2tr}$ . Since  $t_-(0) > r - R + |r - R| > 0$ ,  $-t - \sqrt{\zeta^2 + R^2 + 2tr} < 0$ , hence  $x_-(t) = \sqrt{\zeta^2 + R^2 + 2tr} - t$  or

$$x_{\pm}(t) = \pm \left( t - \sqrt{\zeta^2 + R^2 + 2tr} \right). \quad (\text{E18})$$

Therefore, one concludes that the functions  $y_{\pm}(t)$  are coincident and equal to

$$y_+(t) = y_-(t) = y(t) = \left[ 2t \left( \sqrt{\zeta^2 + R^2 + 2tr} - r \right) - t^2 - \zeta^2 \right]^{1/2} \quad (\text{E19})$$

and.

$$g_3(r, \zeta) = \int_{t_-(0)}^{t_+(0)} \frac{dt}{t} y(t). \quad (\text{E20})$$

Introducing new variable,

$$u = \sqrt{\zeta^2 + R^2 + 2tr} - r, \quad (\text{E21})$$

for which

$$u[t_{\pm}(0)] \equiv u_{\pm} = \sqrt{\zeta^2 + (r \pm R)^2}, \quad (\text{E22a})$$

$$y(t) = \frac{\sqrt{q(u^2)}}{2r}, \quad (\text{E22b})$$

$$q(\eta) = \{u_+^2 - \eta\} \{\eta - u_-^2\}, \quad (\text{E22c})$$

$$dt = \frac{u+r}{r} du \quad (\text{E22d})$$

and so

$$g_3(r, \zeta) = I + I', \quad (\text{E23a})$$

$$I = \int_{u_-}^{u_+} \frac{du}{\sqrt{q(u^2)}} J(u), \quad (\text{E23b})$$

$$J(u) = \frac{q(u^2)(r^2 - \zeta^2 - R^2 - u^2)}{w(u^2)}, \quad (\text{E23c})$$

$$I' = \frac{1}{2r} \int_{u_-^2}^{u_+^2} d\eta J'(\eta), \quad (\text{E23d})$$

$$J'(\eta) = \frac{(\eta - \zeta^2 - R^2 - r^2)}{\sqrt{q(\eta)}w(\eta)}, \quad (\text{E23e})$$

$$w(\eta) = (\eta - \eta_1)(\eta - \eta_2), \quad (\text{E23f})$$

$$\eta_{1,2} = \left( r \pm \sqrt{\zeta^2 + R^2} \right)^2. \quad (\text{E23g})$$

Using equality

$$w(\eta) + q(\eta) = -4r^2\zeta^2, \quad (\text{E24})$$

one can show that the integrand  $J'(\eta)$  is an antisymmetric function with respect to the middle point  $\eta = \{u^2[t_+(0)] + u^2[t_-(0)]\}/2$ , and, therefore, the term (E23d) is equal 0. At the same time, expanding  $J(u)$  into partial fractions, one obtains

$$g_3(r, \zeta) = (R^2 + \zeta^2 - r^2) I_1 + I_2 + I_{3+} + I_{3-}, \quad (\text{E25a})$$

$$I_1 = \int_{u_-}^{u_+} \frac{du}{\sqrt{q(u^2)}}, \quad (\text{E25b})$$

$$I_2 = \int_{u_-}^{u_+} \frac{duu^2}{\sqrt{q(u^2)}}, \quad (\text{E25c})$$

$$I_{3\pm} = 2r\zeta^2 \left( r \pm \sqrt{\zeta^2 + R^2} \right) \int_{u_-}^{u_+} \frac{du}{\sqrt{q(u^2)}(u^2 - \eta_{1,2})} \quad (\text{E25d})$$

The integrals (eqs. E25), one can compute using the substitution

$$u = \sqrt{u_+^2 - (u_+^2 - u_-^2) \sin^2 \phi} \quad (\text{E26})$$

Finally, one arrives at the following expression for the axial component of the cylinder's field

$$\delta g_3(r, z) = 2G\rho g_3(r, \zeta) \Big|_{\zeta=z-h}^{\zeta=z}, \quad (\text{E27a})$$

$$g_3(r, \zeta) = \frac{(\zeta^2 + R^2 - r^2)}{\sqrt{\zeta^2 + (r+R)^2}} K(k) + \sqrt{\zeta^2 + (r+R)^2} E(k) + \frac{\zeta^2}{\sqrt{\zeta^2 + (r+R)^2}} \sum_{j=\pm 1} \left[ \frac{r + j\sqrt{\zeta^2 + R^2}}{R - j\sqrt{\zeta^2 + R^2}} \Pi \left( \frac{2R}{R - j\sqrt{\zeta^2 + R^2}} \middle| k \right) \right], \quad (\text{E27b})$$

$$k = \sqrt{\frac{4rR}{\zeta^2 + (r+R)^2}}, \quad (\text{E27c})$$

where  $K(k)$ ,  $E(k)$  and  $\Pi(\alpha|k)$  are the complete elliptic integrals of the first, second and third order respectively.

## 2. Radial component

For the radial component of the gravitational field  $\delta g_r(r, z) = -\partial_r \Phi(r, z)$  one obtains from (eq. E11)

$$\delta g_r(r, z) = 2G\rho g_r(r, \zeta)_{\zeta=z-h}^{\zeta=z}, \quad (\text{E28a})$$

$$g_r(r, \zeta) = -\int_0^R y \left( \frac{dt_+}{t_+} - \frac{dt_-}{t_-} \right), \quad (\text{E28b})$$

$$t_{\pm}(y) = \zeta + \left[ \zeta^2 + r^2 + R^2 \pm 2r\sqrt{R^2 - y^2} \right]^{1/2} \quad (\text{E28c})$$

Since still  $t_+(R) = t_-(R) \leq t_{\pm}(0)$ , one gets,

$$g_r(r, \zeta) = \int_{t_-(0)}^{t(R)} \frac{dt}{t} y_-(t) + \int_{t(R)}^{t_+(0)} \frac{dt}{t} y_+(t), \quad (\text{E29})$$

where  $y_{\pm}(t)$  are functions inverse to (eq. E28c). Since these functions are the same

$$y_+(t) = y_-(t) \equiv y(t) = \frac{1}{2r} \left[ 4r^2 R^2 - (t^2 - 2\zeta t - r^2 - R^2)^2 \right]^{1/2}, \quad (\text{E30})$$

then, choosing as an integration variable  $u = t - \zeta$ , one finds that

$$g_r(r, \zeta) = I + I', \quad (\text{E31a})$$

$$I = -\frac{\zeta}{2r} \int_{u_-}^{u_+} \frac{du q(u^2)}{(u^2 - \zeta^2) \sqrt{q(u^2)}}, \quad (\text{E31b})$$

$$I' = \frac{1}{4r} \int_{u_-^2}^{u_+^2} \frac{d\eta \sqrt{q(\eta)}}{(\eta - \zeta^2)}, \quad (\text{E31c})$$

where  $u_{\pm}$  and  $q(\eta)$  are given by (eqs. E22a, E22c). Because  $u_{\pm}^2 - \zeta^2$  and  $q(\eta + \zeta^2)$  are independent of  $\zeta$ , the term  $I'$  gives no contribution to the acceleration (eq. E28a) and can be omitted. While using the substitution (eq. E26), one reduces the integral in (eq. E31b) to elliptic integrals, which brings us to the next final result

$$\delta g_r(r, z) = 2G\rho g_r(r, \zeta)_{\zeta=z-h}^{\zeta=z}, \quad (\text{E32a})$$

$$g_r(r, \zeta) = \frac{\zeta}{2r\sqrt{\zeta^2 + (r+R)^2}} \left[ -(\zeta^2 + 2r^2 + 2R^2) K(k) + (\zeta^2 + (r+R)^2) E(k) + \frac{(r^2 - R^2)^2}{(r+R)^2} \Pi\left(\frac{4rR}{(r+R)^2} | k\right) \right], \quad (\text{E32b})$$

where  $k$  is given by (eq. E27c).

- [1] Rosi G, Sorrentino F, Cacciapuoti L, Prevedelli M and Tino G M 2014 *Nature* **510**, 518
- [2] Rosi G 2018 *Metrologia* **55**, 50
- [3] Dubetskii B Ya, Kazantsev A P, Chebotayev V P, Yakovlev V P, 1984 *Pis'ma Zh. Eksp. Teor. Fiz.* **39**, 531 [*JETP Lett.* **39**, 649].
- [4] Tino G M and Kasevich M A (Eds.) 2014 *Atom Interferometry*, Proceedings of the International School of Physics "Enrico Fermi", Volume 188, IOS Press
- [5] Canuel B. et al, 2020 arXiv:2007.04014v1 [physics.atom-ph]
- [6] Ming-Sheng Zhan et al, 2020 *International Journal of Modern Physics D*, **29**, 1940005.
- [7] Badurina L. et al JCAP05(2020)011
- [8] Battelier B. et al, 2019 arXiv:1908.11785v3 [physics.space-ph]
- [9] El-Neaj Y. A. et al, 2020 *EPJ Quantum Technology* **7**:6
- [10] Tino G M. et al., 2019, *Eur. Phys. J. D* **73**, 228
- [11] Lamporesi G 2006 Ph.D. thesis University of Florence
- [12] Fixler J B, Foster G T, McGuirk J M and Kasevich M A 2007 *Science* **315**, 74

- [13] Dubetsky B 2017 *Proc. of the MPLP-2016 Conference (Novosibirsk) IOP Conf. Series: Journal of Physics: Conf. Series* **793** 012006
- [14] Dickerson S M, Hogan J M, Sugarbaker A, Johnson D M S and Kasevich M A 2013 *Phys. Rev. Lett.* **111**, 083001
- [15] Kovachy T, Hogan J M, Sugarbaker A, Dickerson S M, Donnelly C A, Overstreet C and Kasevich M A 2015 *Phys. Rev. Lett.* **114** 143004
- [16] Kovachy T, Asenbaum P, Overstreet C, Donnelly C A, Dickerson S M, Sugarbaker A, Hogan J M and Kasevich M A 2015 *Nature* **528**, 530
- [17] Biedermann G W, Wu X, Deslauriers L, Roy S, Mahadeswaraswamy C and Kasevich M A 2015 *Phys. Rev. A* **91**, 033629
- [18] Dubetsky B 2014 Optimization and error model for atom interferometry technique to measure Newtonian gravitational constant (*Preprint* physics.atom-ph/1407.7287v2)
- [19] Snadden M J, McGuirk J M, Bouyer P, Haritos K G and Kasevich M A 1998 *Phys. Rev. Lett.* **81**, 971
- [20] Peters A, Chung K Y and Chu S 1999 *Nature* **400**, 849
- [21] Roura A 2017 *Phys. Rev. Lett.* **118**, 160401
- [22] Seidov Z F, Skvirsky P I 2000 Gravitational potential and energy of homogeneous rectangular parallelepiped (*Preprint* astro-ph/0002496v1)
- [23] Chen Y T, Cook A 1993 *Gravitational experiment in the laboratory* (Cambridge: University Press)
- [24] Nabighian M N 1962 *Geofis. Pura e Appl.* **53**, 45
- [25] Miles D 2018 *Journal of Applied Geophysics* **159**, 621
- [26] Mathai A M, Provost S B 1993 *Quadratic forms in random variables: theory and applications* (New York: Marcel Dekker, INC)
- [27] Schlamminger St, Holzschuh E, Kündig W, Nolting F, Pixley R E, Schurr J, and Straumann U, 2006 *Phys. Rev. D* **74**, 082001.
- [28] Dubetsky B 2019 *Appl. Phys. B* **125**, 187
- [29] Dubetsky B, Libby S B and Berman P 2016 *Atoms* **4**, 14
- [30] Tiesinga E, Mohr P J, Newell D B, and Taylor B N, "Values of Fundamental Physical Constants," [https://physics.nist.gov/cgi-bin/cuu/Value?bg|search\\_for=Newtonian+gravitational+constant%2F+big+G%3A+bg1](https://physics.nist.gov/cgi-bin/cuu/Value?bg|search_for=Newtonian+gravitational+constant%2F+big+G%3A+bg1).
- [31] Angelis M de, Greco F, Pistorio A, Poli N, Prevedelli M, Saccorotti G, Sorrentino F and Tino G M 2011 *Solid Earth Discuss* **3**, 43
- [32] Bradley M P, Porto J V, Rainville S, Thompson J K and Pritchard D E 1999 *Phys. Rev. Lett.* **83**, 4510 (1999).
- [33] This velocity is equal to  $v = gT_a$ , where  $T_a$  is a time between the 1st pulse and the moment when the atoms reach the apogee of their trajectory. According to the data in the successive arXiv copy [34] of the article [1],  $T_a = 166$ ms, while from the article [1] itself, one arrives to another value  $T_a = 154$ Ms. The value  $T_a = 166$ ms is chosen here.
- [34] Rosi G, Sorrentino F, Cacciapuoti L, Prevedelli M and Tino G M 2014 Precision measurement of the Newtonian gravitational constant using cold atoms (*Preprint* physics.atom-ph/1412.7954)
- [35] Kasevich M A and Dubetsky B 2005 *US Patent* 7,317,184
- [36] Beausoleil R G, Hansch T W 1986 *Phys. Rev. A* **33**, 1661
- [37] Perrin I, Bernard J, Bidet Y, Zahzam N, Blanchard C, Bresson A, Cadoret M 2019 (*Preprint* physics.atom-ph/1907.04403)
- [38] Rosi G, Cacciapuoti L, Sorrentino F, Menchetti M, Prevedelli M and Tino G. M. 2015 *Phys. Rev. Lett.* **114**, 013001
- [39] Prevedelli M, Cacciapuoti L, Rosi G, Sorrentino F and Tino G M 2014 *Phil. Trans. R. Soc. A* **372**, 20140030